

https://doi.org/10.3799/dqkx.2024.112



泰国东南部黎府带晚三叠世碰撞后火山岩成因及其古特提斯构造意义

闫秋彤¹, 钱鑫^{1*}, 张菲菲², Mongkol Udchachon³, 王逸文¹

1. 中山大学地球科学与工程学院, 广东省地球动力作用与地质灾害重点实验室, 南方海洋科学与工程广东省实验室(珠海), 广东珠海 519082
2. 大陆动力学国家重点实验室, 西北大学地质学系, 陕西西安 710069
3. 玛哈沙拉堪大学生命演化、盆地研究及古生物学卓越中心, 古生物学研究与教育中心, 玛哈沙拉堪府 44150, 泰国

摘要: 泰国位于东古特提斯构造域的核心位置, 保存了多条与古特提斯洋俯冲—碰撞—闭合演化有关的构造岩浆岩带。但目前对于其中黎府带早中生代火山岩的研究仍存在不足, 其相关的岩石成因和构造属性未能得到有效限定。因此, 针对泰国东南部黎府带出露的晚三叠世火山岩开展了详细的岩相学、锆石 U-Pb 年代学、地球化学以及 Sr-Nd-Hf 同位素研究, 并结合区域对比综合分析了东古特提斯构造域晚三叠世岩浆活动及其动力学机制。该套样品包括了玄武岩、流纹岩和英安岩, 锆石 U-Pb 定年表明其形成年龄为晚三叠世(204~200 Ma)。其中玄武岩样品具有富铯玄武岩的特征, 其对应的 $(^{87}\text{Sr}/^{86}\text{Sr})_i = 0.70398 \sim 0.70400$, $\epsilon_{\text{Nd}}(t) = +5.0 \sim +5.3$, $\epsilon_{\text{Hf}}(t) = +0.3 \sim +15.5$ 。长英质火山岩样品具有 A 型特征, 且与玄武岩样品具相似的同位素组成, 其对应的 $(^{87}\text{Sr}/^{86}\text{Sr})_i = 0.70271 \sim 0.70472$, $\epsilon_{\text{Hf}}(t) = +4.0 \sim +4.2$, $\epsilon_{\text{Nd}}(t) = +6.8 \sim +16.0$ 。地球化学特征表明该套玄武岩样品来自类似 OIB 特征的亏损软流圈地幔源区, 而长英质火山岩可能来自该套新底侵的基性岩经低程度部分熔融。区域对比表明该套晚三叠世火山岩形成于古特提斯洋碰撞后伸展背景, 是东古特提斯洋碰撞闭合后最晚期的岩浆活动。年代学数据对比显示黎府带与清孔—南邦—塔克火山岩带均具有相似的三叠纪年龄谱系, 证实了在中-晚三叠世时期黎府带也同样记录了东古特提斯洋碰撞及碰撞后的岩浆作用。

关键词: 泰国东南部; 黎府带; 晚三叠世; 碰撞后岩浆作用; 东古特提斯洋; 岩石学; 构造。

中图分类号: P581

文章编号: 1000-2383(2025)06-2144-19

收稿日期: 2024-08-22

Petrogenesis of Late Triassic Post-Collisional Volcanic Rocks from Loei Zone in Southeastern Thailand and Its Paleotethyan Tectonic Implications

Yan Qiutong¹, Qian Xin^{1*}, Zhang Feifei², Mongkol Udchachon³, Wang Yiwen¹

1. Guangdong Key Lab of Geodynamics and Geohazards, School of Earth Sciences and Engineering, Sun Yat-sen University, Southern Marine Science and Engineering, Guangdong Laboratory (Zhuhai), Zhuhai 519082, China
2. State Key Laboratory of Continental Dynamics, Department of Geology, Northwest University, Xi'an 710069, China

基金项目: 国家自然科学基金项目(Nos.42330302,42172235); 南方海洋科学与工程广东省实验室(珠海)(No.SML2023SP239)。

作者简介: 闫秋彤(2001—), 女, 硕士研究生, 岩石学矿物学矿床学专业。ORCID: 0009-0000-5429-2668。E-mail: yanqt3@mail2.sysu.edu.cn

* **通讯作者:** 钱鑫, 教授, 博士生导师, 从事东南亚大地构造研究。ORCID: 0000-0002-3587-861X。E-mail: qianx3@mail.sysu.edu.cn

引用格式: 闫秋彤, 钱鑫, 张菲菲, Mongkol Udchachon, 王逸文, 2025. 泰国东南部黎府带晚三叠世碰撞后火山岩成因及其古特提斯构造意义. 地球科学, 50(6): 2144-2162.

Citation: Yan Qiutong, Qian Xin, Zhang Feifei, Mongkol Udchachon, Wang Yiwen, 2025. Petrogenesis of Late Triassic Post-Collisional Volcanic Rocks from Loei Zone in Southeastern Thailand and Its Paleotethyan Tectonic Implications. *Earth Science*, 50(6): 2144-2162.

3. Center for Excellence on the Evolution of Life, Basin Studies and Applied Paleontology, Palaeontological Research and Education Center, Mahasarakham University, Maha Sarakham 44150, Thailand

Abstract: Thailand is located in the core region of the East Paleotethyan Domain, preserves numerous tectonic-magmatic belts related to the subduction-collision-closure evolution of the Paleotethyan Ocean. However, the study on the Early-Middle Mesozoic volcanic rocks in the Loei zone remains unclear and the related petrogenesis and tectonic setting have not been constrained. Therefore, this study carries out detailed petrographic, zircon U-Pb geochronology, geochemistry and Sr-Nd-Hf isotopic studies on the Late Triassic volcanic rocks along the Loei zone in southeastern Thailand. Our study along with regional comparisons comprehensively analyze the Late Triassic magmatism and geodynamics process in the East Paleotethyan Domain. The study samples include basalts, rhyolites and dacites, with Late Triassic zircon U-Pb ages of 204–200 Ma. The basalts exhibit characteristics of Nb-enriched basalts, with $(^{87}\text{Sr}/^{86}\text{Sr})_i = 0.703\ 98 - 0.704\ 00$, $\epsilon_{\text{Nd}}(t) = +5.0 - +5.3$, $\epsilon_{\text{Hf}}(t) = +0.3 - +15.5$. The felsic volcanic samples exhibit A-type characteristics and share similar isotopic compositions with the basalt samples, with $(^{87}\text{Sr}/^{86}\text{Sr})_i = 0.702\ 71 - 0.704\ 72$, $\epsilon_{\text{Nd}}(t) = +4.0 - +4.2$, $\epsilon_{\text{Hf}}(t) = +6.8 - +16.0$. Geochemical characteristics indicate that these basalts originated from a depleted OIB-like asthenospheric mantle source, while the felsic volcanic rocks possibly originated from the low level partial melting of these newly underplated mafic rocks. Regional comparisons indicate that these Late Triassic volcanic rocks were formed in a post-collisional extensional setting, representing the latest magmatism after the collision and closure of the East Paleotethyan Ocean. Comparison of chronological data shows that the Loei zone and the Chiang Khong-Lampang-Tak zones share similar Triassic age-spectra pattern, confirming that the Loei zone also recorded the collisional and post-collisional magmatism related to the Eastern Paleotethyan evolution during the Middle-Late Triassic.

Key words: southeastern Thailand; Loei zone; Late Triassic; post-collisional magmatism; East Paleotethyan Ocean; petrology; tectonic.

0 引言

古特提斯洋是早古生代至早中生代存在于冈瓦纳大陆和劳亚大陆之间的古大洋,该大洋西起现今阿尔卑斯途经中亚、西藏、滇西并南延至东南亚等地,其中滇西和东南亚地区隶属于该构造域的东段,是古特提斯洋构造演化地质记录保存最为完整的地区(如 Metcalfe, 1996, 2006, 2011, 2013, 2021; 钟大赉, 1998; Yin and Harrison, 2000; Ca-wood *et al.*, 2007; Sone and Metcalfe, 2008; Oliver *et al.*, 2014; Wang *et al.*, 2018, 2022; Qian *et al.*, 2019; Song *et al.*, 2020; 吴福元等, 2020; Fan *et al.*, 2024)。以往的研究表明东古特提斯构造带经过了缅甸东部、泰国北部以及老挝西部并向南可进一步延伸至马来半岛及印尼邦加岛—勿里洞岛等地区,并系统记录了东古特提斯洋演化过程中有关的构造、岩浆、变质和沉积记录(如 Sone *et al.*, 2012; Qian *et al.*, 2015, 2020, 2021, 2022; Wang *et al.*, 2016, 2021a; Zhao *et al.*, 2016; Zhang *et al.*, 2019; 徐畅等, 2020; 余小清等, 2021; Yu *et al.*, 2022, 2023; 李慧玲等, 2023; Hara *et al.*, 2024)。

泰国地处东古特提斯构造域的核心部位,由西

部的滇缅马陆块和东部的印支陆块所组成,区域内由西向东包括了清迈—清莱带、素可泰带、难河带和黎府带(图 1a),以往的研究在这些构造带识别出了与古特提斯洋构造演化相关的俯冲、碰撞和碰撞后的岩浆及沉积作用(如 Charusiri *et al.*, 1993, 2002; Ueno and Hisada, 2001; Metcalfe, 2002, 2013; Sone *et al.*, 2012; Qian *et al.*, 2013, 2017b, 2022; Wang *et al.*, 2020)。其中素可泰岛弧带包括了清孔—南邦—塔克火山岩带和中部及东部两个花岗岩亚省,为中—晚三叠世东古特提斯洋俯冲—碰撞作用的产物,带内出露的平行于缝合带展布的中—酸性火山岩均认为代表了古特提斯洋由俯冲向碰撞转换及碰撞后两期主要的岩浆作用,其向北可以与滇西的临沧带相连(如 Barr *et al.*, 2000, 2006; Metcalfe, 2011; Wang *et al.*, 2016, 2017; Qian *et al.*, 2017a)。难河构造带是素可泰岛弧带与印支陆块的分界,被认为是古特提斯洋弧后盆地的残余(如 Ueno and Charoentitirat, 2011; Qian *et al.*, 2015, 2016b; Yang *et al.*, 2016; Wang *et al.*, 2020)。

泰国境内黎府带主要出露于碧差汶和黎府等地区,向北被认为可以延伸至老挝西部地区,是东南亚重要的铜—金多金属成矿带(Qian *et al.*,

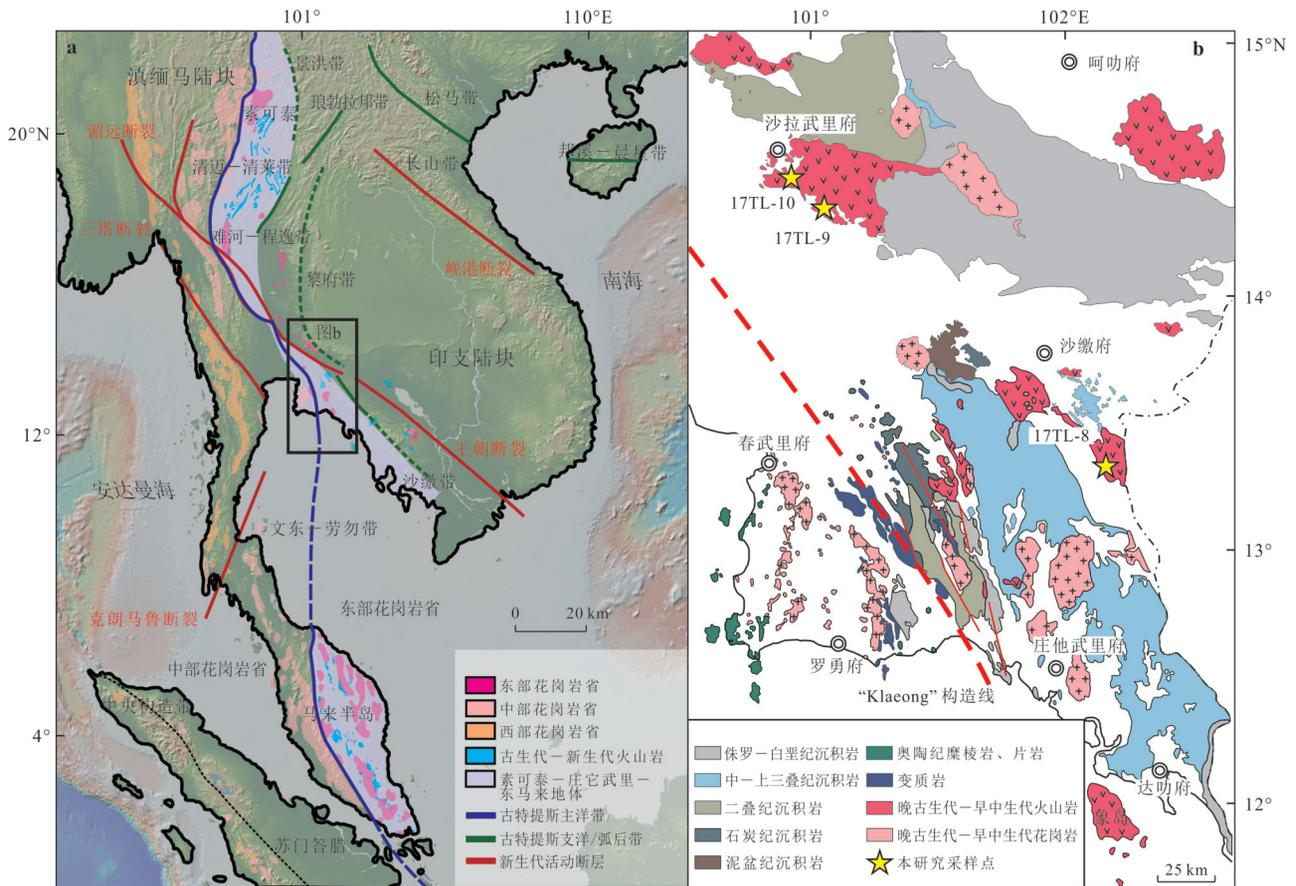


图 1 东南亚地区区域构造图(a)和研究区地质简图(b)

Fig.1 Regional tectonic framework (a) and simplified geological map of study area (b)

图 a 据 Wang *et al.* (2018); 余永琪等 (2024); 图 b 据 Qian *et al.* (2022)

2015; Guo *et al.*, 2024). 但是以往对该带的研究主要集中在晚古生代岛弧岩浆作用及与成矿关系上, 缺少对中生代时期岩浆作用及构造属性的研究, 此外该带与清迈—南邦—塔克火山岩带的关系也未能得到有效限定(如 Barr *et al.*, 2000, 2006; Srichan *et al.*, 2009; Qian *et al.*, 2013, 2015, 2016a, 2016b, 2017a, 2017b, 2021, 2022; Kamvong *et al.*, 2014; Salam *et al.*, 2014; Arboit *et al.*, 2016; Fanka *et al.*, 2016; Yang *et al.*, 2016; Shi *et al.*, 2019, 2021; Wang *et al.*, 2020; Jin *et al.*, 2024).

因此为解决上述问题, 本研究对泰国东南部黎府带开展了详细的野外地质调查和样品采集, 并于泰国沙缴府、庄他武里府和沙拉武里府地区新识别出一套保存完好的晚三叠世火山岩组合(图 1b). 针对其中的粗面玄武岩、流纹岩和英安岩样品开展了详细的锆石 U-Pb 年代学、锆石原位 Hf 同位素、全岩主—微量元素和 Sr-Nd 同位素的分析研究, 并结合收集到的黎府带及其周缘火山岩带年代学和地球

化学数据进行综合的对比与讨论, 为探究黎府带晚三叠世岩浆作用特征及其构造演化提供新的约束.

1 地质概况与岩相学特征

泰国地处中南半岛的核心部位, 区域内主要包含了滇缅马陆块和印支陆块两大构造单元, 它们被清迈—清莱东古特提斯带所分隔(如 Metcalfe, 2011; Sone *et al.*, 2012; Wang *et al.*, 2018). 其中位于泰国西部的滇缅马陆块在早二叠世与冈瓦纳大陆分离, 陆块内发育了冰碛砾岩和泥岩且保存有冷水相的动物群, 这些特征表明该陆块具有冈瓦纳大陆的亲缘性(如聂泽同等, 1997; Ueno and Charoentitirat, 2011). 而位于泰国东部的印支陆块在泥盆纪就与冈瓦纳大陆分离, 陆块内发育有石炭纪—二叠纪热带—亚热带古动植物群, 具有华夏陆块的亲缘性(如 Metcalfe, 2000; Hutchison and Tan, 2009).

清迈—清莱带位于泰国西北部, 带内出露有远

洋放射虫硅质岩、高级变质岩、寒武纪砂岩、奥陶纪灰岩及石炭—二叠纪蛇绿混杂岩等(如 Ueno and Hisada, 2001; Feng *et al.*, 2004, 2008; Ridd *et al.*, 2011; Ridd, 2015; Wang *et al.*, 2016). 此外带内还存留了较为完整的上泥盆统牙形石动物群及覆盖于碱性洋岛玄武岩之上的浅水含虫链碳酸盐岩(如 Ueno *et al.*, 2003; Ueno and Charoentitirat, 2011; Wang *et al.*, 2017). 该带进一步向南可与马来半岛内的文冬—劳勿带相连,代表了东古特提斯洋主洋盆的缝合位置(图 1a; Ueno and Hisada, 2001; Wang *et al.*, 2018, 2021b; Zhang *et al.*, 2023).

素可泰地体是古特提斯洋向印支陆块俯冲过程中的岛弧系统,主要分布有石炭—三叠纪陆源碎屑岩和岛弧火山岩(如 Barr *et al.*, 2000; Metcalfe, 2011, 2013; Qian *et al.*, 2013, 2017a). 难河—沙缴带可延伸至柬埔寨贡布省,带内主要出露了早二叠—中三叠世放射虫硅质岩及蛇绿混杂岩带,已有的研究表明其中的基性火山岩形成于 315 Ma,且具有弧后盆地的地球化学特征(如 Qian *et al.*, 2015; Yang *et al.*, 2016; Wang *et al.*, 2020). 黎府带向北可延伸至老挝中部,向东可延伸至柬埔寨西部,前人研究表明在该构造带存在晚泥盆—石炭纪和晚二叠—三叠纪两期较为集中的弧岩浆作用(如 Barr and Charusiri, 2011; Salam *et al.*, 2014; Qian *et al.*, 2016a, 2016b).

本次研究区位于泰国东南部沙拉武里府至庄他武里府地区,区域内出露最老的地层为前志留系 Na Mo 群,主要由变形程度较为明显的低绿片岩相岩石组成(Bunopas, 1981). 志留纪至白垩纪地层分布较为广泛且时代连续,其中志留纪—泥盆纪地层主要出露砂岩、泥岩、层状硅质岩等,且在硅质岩中发现了晚泥盆世—早石炭世的放射虫化石(Sashida *et al.*, 1993). 石炭纪地层主要出露在呵叻高原西缘,主要由近岸砂岩、页岩和灰岩构成,可见有孔虫化石(Chairangsee *et al.*, 1990). 二叠纪—早三叠世地层属于浅海沉积单元,包含页岩、砂岩和石灰岩等,且在中二叠世地层中发现了双壳类动物群,而中晚三叠世地层主要为深海沉积单元(Feng *et al.*, 2009; Udchachon *et al.*, 2024). 侏罗—白垩纪地层分布于帕府和呵叻高原等地区,以一套由页岩、砂岩、砾岩和黏土岩组成的红层陆相碎屑岩沉积为特征(Charusiri *et al.*, 1993).

如前所述泰国地区的黎府带火山岩主要出露

于黎府和碧差汶地区,主要由泥盆—石炭纪和二叠—三叠纪的安山岩和流纹岩组成,可见少量玄武岩和斑岩,该带的岩浆活动时间在二叠—三叠纪较为活跃,向南认为可以与那空他地区出露的二叠至三叠纪中酸性火山岩相连,其年龄主要集中于 294~207 Ma(如 Kamvong *et al.*, 2014; Salam *et al.*, 2014; Qian *et al.*, 2015, 2022; Arboit *et al.*, 2016; Fanka *et al.*, 2016; Shi *et al.*, 2019, 2021; Wang *et al.*, 2020).

本研究样品采自泰国东南部黎府带南部地区,其中粗面玄武岩样品 17TL-8 采于沙缴府与庄他武里府的交界地区(N13°20'08.04", E102°10'15.21") (图 1b),样品呈灰绿色(图 2a),镜下可见斑状结构,斑晶主要为斜长石和辉石,其中斜长石发育聚片双晶,基质由微晶斜长石和少量辉石所组成,部分辉石可见绿泥石化现象(图 2d). 流纹岩样品 17TL-9 采于沙缴府 Nan Bang 北部与沙拉武里府交界处 3222 号公路旁(N14°22'42.98", E101°05'32.36"),呈浅灰色出露,显微镜下观察样品具有斑状结构,斑晶主要由石英(20%~25%)和透长石(5%~10%)组成,基质由玻璃质组成(图 2e). 英安岩样品 17TL-10 采于沙拉武里府 Pholoyothin Rd 高速路天桥旁(N14°29'18.83", E100°54'55.79"),呈现深灰色,镜下观察样品具有斑状结构,斑晶以斜长石(10%~20%)和石英(20%~25%)为主,可见其熔蚀反应边结构(图 2f).

2 分析方法

2.1 锆石 U-Pb 定年及原位 Lu-Hf 同位素测定

本文将采集到的样品通过重液法和磁选法分选锆石颗粒,利用双筒体视显微镜挑选出其中无色干净、无明显裂纹、晶形较好的锆石,并将其固定于环氧树脂靶上并抛光至锆石中心位置. 锆石 U-Pb 同位素定年分析在中山大学地球动力作用与地质灾害广东省重点实验室使用激光剥蚀系统与电感耦合等离子体质谱仪联用(LA-ICP-MS)完成. ICP-MS 型号为 iCAP RQ,分析采用的激光束斑直径和频率分别为 32 μm 和 5 Hz,详细的测试过程参考 Wang *et al.* (2020). 选取锆石标样 91500(1 062.4 \pm 0.6 Ma)和玻璃标准物质 NIST610 用于 U-Pb 同位素分馏校正. 对原始数据用软件 GLITTER(Griffin *et al.*, 2008)进行分析处理,用 ISOPLOT 软件对锆石 U-Pb 年龄进行谐和图的绘制并对年龄加权平均



图2 泰国东南部黎府带火山岩野外露头(a~c)和正交偏光镜下显微岩相学特征(d~f)

Fig.2 Field photo (a~c) and photomicrographs (d~f) for the volcanic rocks in the Loei zone of SE Thailand

矿物缩写: Pl. 斜长石; Qtz. 石英; Cpx. 辉石; Chl. 绿泥石

值(Ludwig, 2001)进行计算. 锆石原位 Lu-Hf 同位素分析在中山大学广东省地球动力作用与地质灾害重点实验室进行, 将 Neptune Plus 型多接收电感耦合等离子体质谱(MC-ICP-MS)和 Geolas HD 型 193 nm Ar F 激光剥蚀系统联合使用完成测试. 详细的分析过程参考 Hu *et al.* (2012). 采用标准锆石样品 91500 和 Plešovice 校正同位素的分馏校正并监测仪器状态. 计算 $\epsilon_{\text{Hf}}(t)$ 的各项参数中 ^{176}Lu 的衰变常数选用 $1.867 \times 10^{-11} \text{a}^{-1}$ (Scherer *et al.*, 2001), 现今球粒陨石的 $^{176}\text{Hf}/^{177}\text{Hf}$ 和 $^{176}\text{Lu}/^{177}\text{Hf}$ 值选用 0.282 772 和 0.033 2 (Blichert-Toft and Albarede, 1997), 亏损地幔的 $^{176}\text{Hf}/^{177}\text{Hf}$ 值选用 0.283 250 (Vervoort *et al.*, 1999).

2.2 全岩主、微量元素及 Sr-Nd 同位素分析

将代表性样品粉碎至 200 目进行全岩主微量元素和 Sr-Nd 同位素测试, 测试均在中山大学地球科学与工程学院广东省地球动力作用与地质灾害重点实验室完成. 使用 ARL Perform'X 4200 型 X 射线荧光光谱仪(XRF)进行全岩主量元素测试, 选用熔片法进行样品制备, 称量烘干后的样品和硼酸锂混合熔剂称量至坩埚中, 加入饱和碘化铵(NH_4I)溶液, 放入铂金坩埚中加热至 1 050 °C 共熔制片, 分析精度优于 5%, 详细的实验方法见 Wang *et al.* (2020). 全岩微量元素溶液分析使用 Thermo Scien-

tific iCAP-RQ-ICP-MS 进行, 分析精度优于 5%, 详细的实验方法见 Wang *et al.* (2020). Sr-Nd 同位素测试使用 Neptune Plus 型多接收电感耦合等离子体质谱仪(MC-ICP-MS)完成, 采用国际标准 NIST NBS-987 对样品 Sr、Nd 同位素比值进行监控, 测定过程中采用 $^{86}\text{Sr}/^{88}\text{Sr}=0.119 4$ 和 $^{146}\text{Nd}/^{144}\text{Nd} = 0.721 9$ 进行分馏校正, 详细分析测试流程见 Yang *et al.* (2006).

3 分析结果

3.1 锆石 U-Pb 年代学及原位 Hf 同位素特征

本研究对泰国东南部黎府带的粗面玄武岩样品(17TL-8-6, 17TL-8-10)和长英质火山岩样品(17TL-9-1, 17TL-9-6, 17TL-10-1)开展了详细的 LA-ICP-MS 锆石 U-Pb 年代学分析和原位 Lu-Hf 同位素分析, 分析结果见附表 1 和 2.

粗面玄武岩样品 17TL-8-6 和 17TL-8-10 的锆石颗粒多具自形的短柱状无色透明特征. 17TL-8-6 样品中的 5 颗锆石的表观年龄较为接近为 203.2~204.8 Ma, 其 Th/U 比值为 0.71~1.68, 加权平均年龄为 $204.1 \pm 1.3 \text{ Ma}$ (MSWD=0.51; 图 3a). 17TL-8-10 样品中的 10 颗锆石的表观年龄较为接近 (198.4~202.5 Ma), 其 Th/U 比值为 0.46~0.96, 加

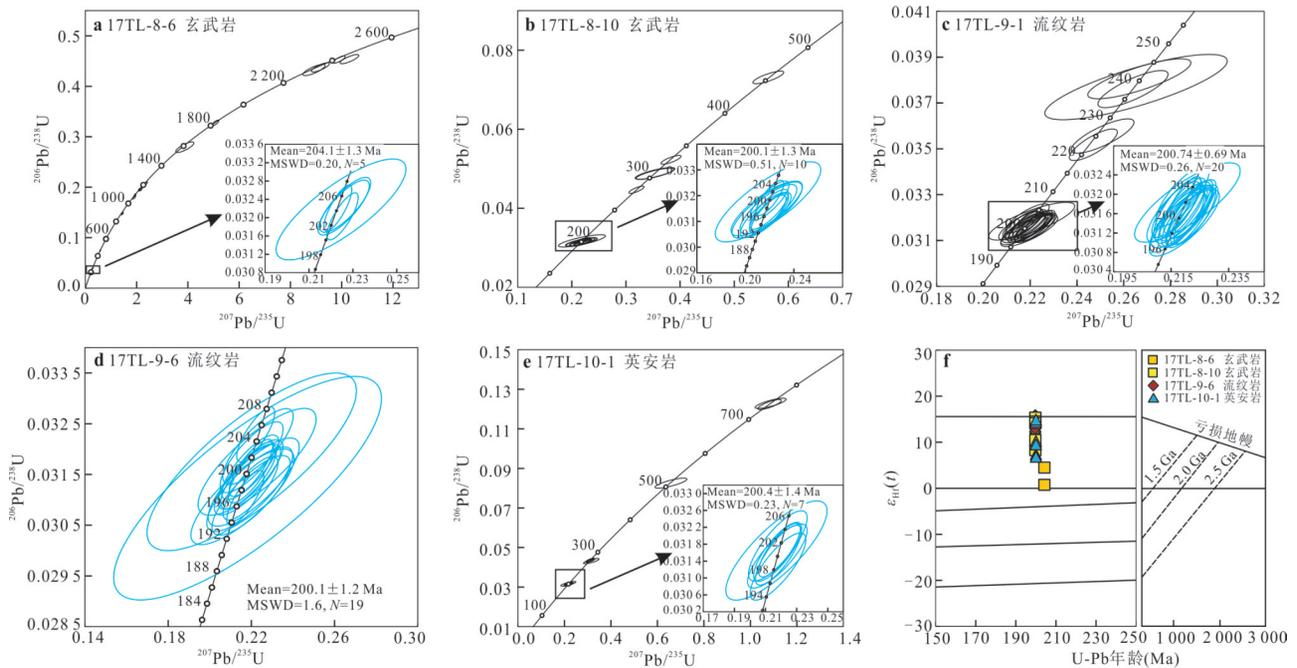


图3 泰国东南部黎府带火山岩锆石 U-Pb 年龄谱和图 (a~e) 和锆石年龄- $\epsilon_{\text{Hf}}(t)$ 图解 (f)

Fig.3 U-Pb concordia diagrams (a~e) and plot of age (Ma) vs. $\epsilon_{\text{Hf}}(t)$ for zircon grains (f) from the volcanic rocks in the Loei zone of SE Thailand

权平均年龄为 200.1 ± 1.3 Ma (MSWD=0.20; 图 3b). 针对两个样品共 12 颗锆石开展了原位 Lu-Hf 同位素组成分析, 测试结果显示两个样品均具有正的 $\epsilon_{\text{Hf}}(t)$ 值, 分别为 $+0.3 \sim +4.1$ 和 $+8.3 \sim +15.5$ (图 3f), 其模式年龄 (T_{DM1}) 分别为 698~859 Ma 和 230~526 Ma.

流纹岩样品 17TL-9-1 和 17TL-9-6 的 Th/U 比值为 0.47~2.50, 39 颗锆石样品的表观年龄集中在 197.1~204.9 Ma, 所得 U-Pb 加权平均年龄分别为 200.74 ± 0.69 Ma (MSWD=0.26) 和 200.1 ± 1.2 Ma (MSWD=1.6) (图 3c~3d). 英安岩样品 17TL-10-1 的 Th/U 比值为 0.04~1.98, 7 颗锆石样品的表观年龄集中在 198.5~201.5 Ma, 其 U-Pb 加权平均年龄为 200.4 ± 1.4 Ma (MSWD=0.26) (图 3e). 针对流纹岩 17TL-9-6 样品的 13 颗锆石和英安岩 17TL-10-1 样品的 7 颗锆石开展了原位 Lu-Hf 同位素组成分析, 结果显示两个样品对应的锆石 $\epsilon_{\text{Hf}}(t)$ 值分别为 $+12.1 \sim +16.0$ 和 $+6.8 \sim +15.0$ (图 3f), 其模式年龄 (T_{DM1}) 年龄分别为 209~366 Ma 和 249~582 Ma.

3.2 岩石地球化学特征

本研究对采自泰国东南部黎府带东南部的 25 件火山岩样品开展了全岩主-微量元素和 Sr-Nd 同位素分析, 详细结果见附表 3.

玄武岩样品具有相对高的烧失量 (LOI) 为

1.87%~4.41%, 但样品的主量元素与烧失量间无明显的线性关系, 表明样品的主量元素受后期蚀变作用的影响较小. 样品的 SiO_2 含量为 48.95%~52.44%, MgO 为 4.49%~7.12%, Al_2O_3 为 13.88%~16.89%, CaO 为 7.15%~10.46%, Fe_2O_3 为 11.00%~13.57%. 在 TAS 和 Co-Th 图解中样品落入粗面玄武岩和钙碱性玄武岩范围内 (图 4a 和 4b). 该组样品具有较高的 Nb 含量为 $9.7 \times 10^{-6} \sim 19.0 \times 10^{-6}$, 在 Nb/U-Nb 图解中落入富铌玄武岩区域 (图 4c). 在哈克图解中样品的 Fe_2O_3 、CaO、 Al_2O_3 和 SiO_2 呈负相关关系, TiO_2 、 Na_2O 和 SiO_2 呈正相关关系, 而 K_2O 、MgO、 P_2O_5 和 SiO_2 无明显相关关系 (附图 1). 长英质火山岩样品的 LOI 较小为 1.08%~2.95%, 表明样品受后期蚀变作用较弱. 样品具有较高的 SiO_2 (64.44%~70.83%) 和 K_2O (3.75%~4.79%) 含量, 较低的 MgO (0.66%~1.91%), CaO (2.03%~3.49%), Fe_2O_3 (3.62%~5.82%) 和 TiO_2 (0.61%~1.00%) 含量. 在 TAS 和 Co-Th 图解 (图 4a 和 4b) 中样品落在高钾钙碱性英安岩和流纹岩范围, 并可进一步划分为 A2 型 (图 4d 和 4e). 在哈克图解中长英质火山岩主量元素特征总体与黎府带同期火山岩相类似, 样品的 Fe_2O_3 、 Al_2O_3 、 TiO_2 、MgO、 P_2O_5 和 SiO_2 呈负相关关系, 而 CaO、 Na_2O 、 K_2O 和 SiO_2 无明显相关关系 (附图 1).

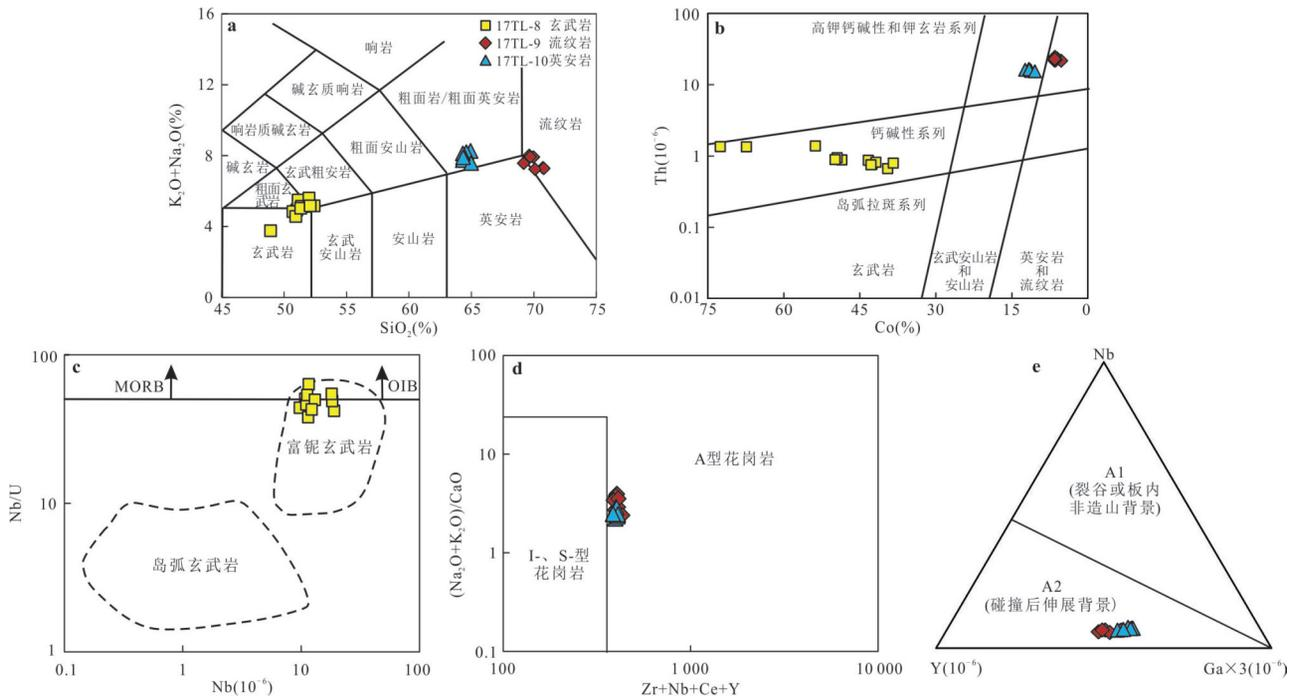


图 4 泰国东南部黎府带火山岩图解

Fig.4 Diagrams for the volcanic rocks in the Loei zone of SE Thailand

a. TAS, 据 Le Maitre *et al.* (1989); b. Co-Th, 据 Hastie *et al.* (2007); c. Nb-Nb/U, 据 Kepezhinskas *et al.* (1996); d. Zr+Nb+Ce+Y-(K₂O+Na₂O)/CaO; e. Nb-Y-Ga

球粒陨石标准化稀土元素配分图显示玄武岩样品轻稀土元素含量高于重稀土元素含量, 无明显的 Eu 异常 (图 5a). 原始地幔标准化微量元素蛛网图显示该组样品均富集高场强元素, 并具有显著的 Nb、Ta、Ti 正异常, 这些特征与典型的富铌玄武岩相似 (图 5b; 如 Aguillón-Robles *et al.*, 2001; Castillo, 2008). 长英质火山岩样品的总稀土元素含量偏高, 具有明显的 Eu 负异常 ($Eu/Eu^+ = 0.59 \sim 0.73$) (图 5c). 原始地幔标准化微量元素蛛网图显示样品以富集大离子亲石元素 (如 Rb、U) 而亏损高场强元素 (如 Nb、Ta、Ti) 为特征, 并具有显著的 Ba、P、Sr 的负异常 (图 5d). 通过数据收集和对比发现, 本文的长英质火山岩具有与黎府带同期火山岩相类似的稀土和微量元素配分模式 (图 5c~5d; Qian *et al.*, 2017a; Nualkhao *et al.*, 2018; Shi *et al.*, 2019, 2021; Uchida *et al.*, 2022, 2023).

玄武岩样品的初始 ($^{87}\text{Sr}/^{86}\text{Sr}$)_i 范围为 0.703 98~0.704 00, $\epsilon_{\text{Nd}}(t)$ 为 +5.0~+5.3. 而长英质火山岩样品具有相类似的初始 ($^{87}\text{Sr}/^{86}\text{Sr}$)_i 比值为 0.702 71~0.704 72 和 $\epsilon_{\text{Nd}}(t)$ 值为 +4.0~+4.2. 所以这些火山岩样品的 Sr-Nd 同位素组成均类似区域上晚三叠碰撞后火山岩, 但是明显不同于黎府带内同期花岗

岩, 且更靠近亏损地幔端元 (图 6; Qian *et al.*, 2016a, 2016b, 2017a, 2020; Wang *et al.*, 2018; Uchida *et al.*, 2022, 2023).

4 讨论

4.1 岩石成因

在岩石形成过程中, 分配系数较低的元素 (如 Th、La、Ce、Sm) 在分离结晶过程中浓度变化缓慢, 但在部分熔融过程中变化较大. 本文研究玄武岩样品的 Th/Ce 比值为 0.03~0.04, Th/La 比值为 0.08~0.11, 远低于大陆地壳范围 (Th/Ce = ~0.15, Th/La = ~0.30; Plank, 2005). 在 La/Sm-La 图解中 (图 7a), 样品沿着部分熔融趋势分布. 样品呈现低且变化的 Cr、Ni 和 $\text{Mg}^\#$ 值, 表明这些玄武岩样品在岩浆演化的过程中可能经历了橄榄石和辉石的分离结晶作用. 此外多数样品具有 Sr 和 Eu 的正异常, 这些特征结合 $\text{CaO}/\text{Al}_2\text{O}_3$ 和 $\text{Mg}^\#$ 之间的相关性表明在岩浆演化分异的过程也存在斜长石的分离结晶作用 (图 7b). 深部地幔的岩浆具有较低的 La/Ta 比值 (8~15), 受到岩石圈地幔混染后该比值会迅速上升 ($\text{La}/\text{Ta} > 25$), 而 La/Sm 比值几乎保持不变, 但在受到地壳物质混染后 La/Sm 比值会迅速增

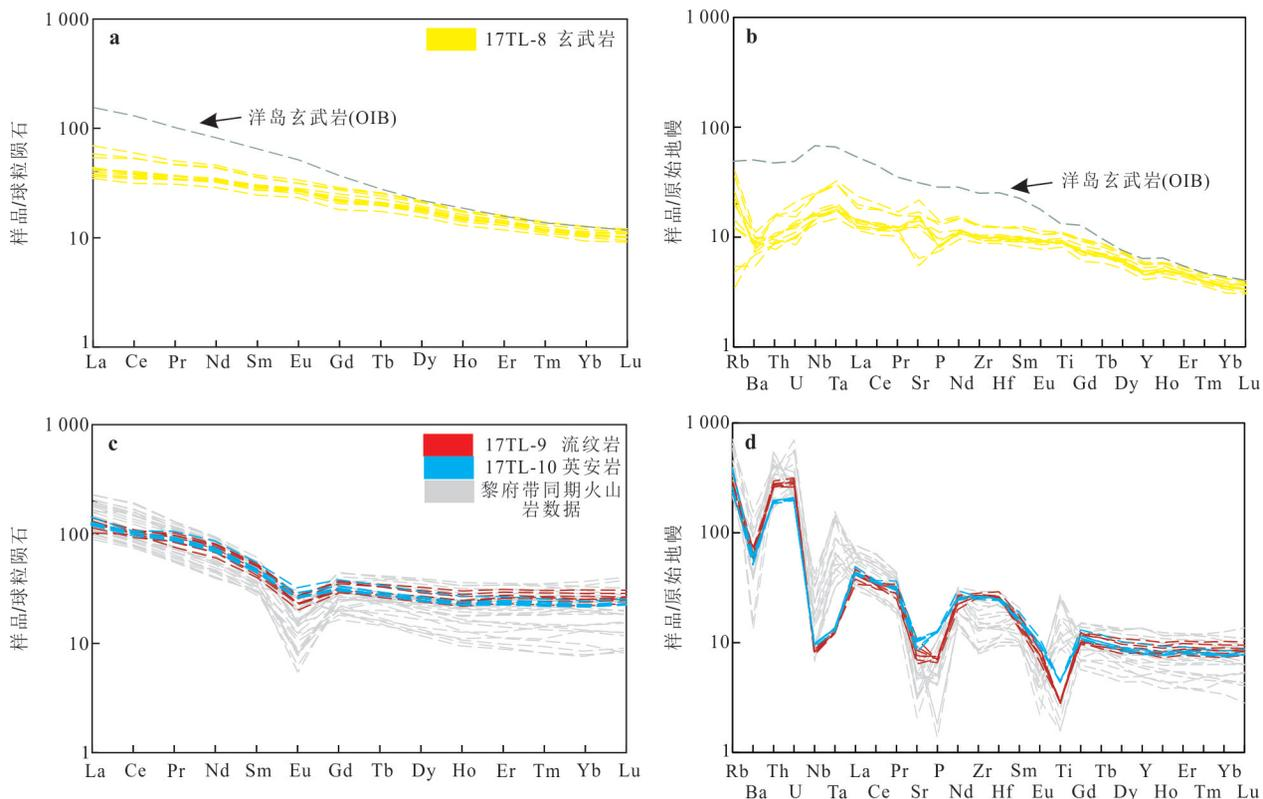


图 5 泰国东南部黎府带火山岩球粒陨石标准化稀土元素配分曲线 (a, c)和原始地幔标准化微量元素蛛网图(b, d)

Fig.5 Primitive mantlenormalized spidergram (a, c) and Chondritenormalized REE pattern (b, d) for the volcanic rocks in the Loei zone of SE Thailand

背景数据引自 Qian *et al.* (2017a); Nualkhao *et al.* (2018); Shi *et al.* (2019, 2021); Uchida *et al.* (2022, 2023); 球粒陨石和原始地幔标准化数据引自 Sun and McDonough (1989)

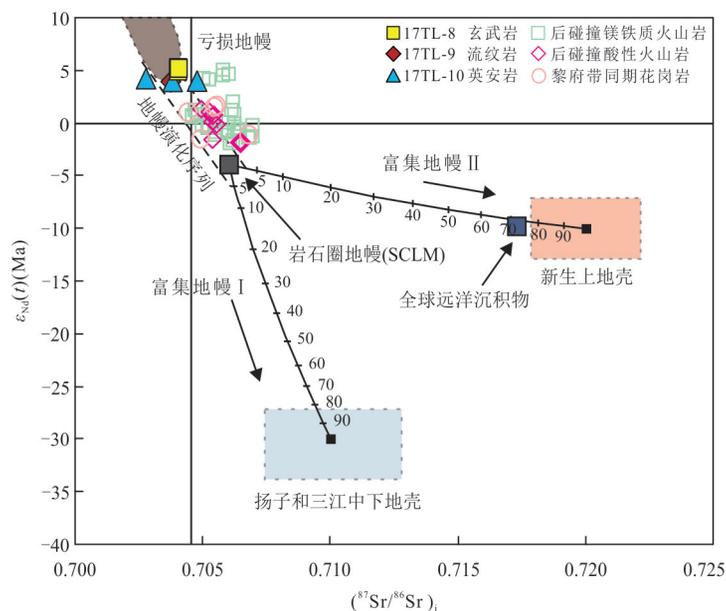


图 6 泰国东南部黎府带火山岩 Sr-Nd 同位素图解

Fig.6 Plot of Sr vs. Nd isotopic data for the volcanic rocks in the Loei zone of SE Thailand

底图据 Zi *et al.* (2012); Qian *et al.* (2021); 背景数据来自 Qian *et al.* (2016a, 2016b, 2017a, 2020); Wang *et al.* (2018); Uchida *et al.* (2022, 2023)及其参考文献

大到 5 以上(如张招崇等, 2004). 如前所述该组样品主要为一套钙碱性的富铈玄武岩, 表现出与洋岛玄武岩相类似的配分模式(图 5a 和 5b), 且具有明显亏损的 Sr-Nd-Hf 同位素组成(图 3f 和图 7), 这些地化特征结合样品较低的 La/Ta 比值(11.04~14.44)和较为稳定的 La/Sm 比值(1.90~2.51), 表明玄武岩样品来自深部地幔而非岩石圈衍生的熔体, 且形成过程中无明显的地壳混染. 在 Th/Ta-Zr 图解中(图 7c), 样品具 OIB 地幔的分布趋势, 进一步说明玄武岩样品主要来自类似 OIB 特征的亏损软流圈地幔源区.

长英质火山岩样品同样相对富集 LREE 和 Rb、U 等大离子亲石元素, 但 Nb、Ta、Ti 等高场强元素相对亏损且具有明显的 Eu 负异常, 表明在岩浆演化过程中存在斜长石的分离结晶. 此外样品具有较高的 $\text{Na}_2\text{O}+\text{K}_2\text{O}$ 值、Ga/Al 和 FeOt/MgO 比值且富集 Zr、Nb 和 REE 元素, 这些特征和典型的 A 型花岗岩相似, 在图 4d 中样品也集中落入了 A 型花岗岩区域(如 Whalen *et al.*, 1987). A 型花岗岩与 I 型和 S 型花岗岩相较具有较高的形成温度(如 Collins *et al.*, 1982), 通过计算研究得出该套长英质火山岩样品

的锆石饱和温度在 805~836 °C(平均温度为 821 °C), 这个温度高于 S 型花岗岩的平均温度 764 °C 和 I 型花岗岩的平均温度 781 °C(King *et al.*, 1997; 刘昌实等, 2003). 因此, 上述特征均表明本研究长英质火山岩样品具有 A 型花岗岩的特征.

目前对于具有 A 型特征的长英质火山岩的成因主要包括了: (1) 下地壳镁铁质岩石的部分熔融(Whalen *et al.*, 1987; Frost and Ronald Frost, 1997; 张旗和李承东, 2012); (2) 地幔碱性玄武质岩浆的分离结晶作用(Vander Auwera *et al.*, 2003; Namur *et al.*, 2011); (3) 幔源碱性岩浆与地壳来源花岗岩岩浆的混合作用(Kerr and Fryer, 1993; Mingram *et al.*, 2000). 如前所述长英质火山岩样品具有相对较高的 SiO_2 (64.44%~70.83%) 和较低的 MgO (0.66%~1.91%), $\text{Fe}_2\text{O}_3\text{t}$ (3.62%~5.82%) 和 TiO_2 (0.61%~1.00%) 含量, 富集大离子亲石元素(图 5c 和 5d), 这些特征与幔源岩浆作用的产物不相符. 在图 7d 中, 该套长英质火山岩均落入贫粘土物质源区并靠近玄武质派生熔体端元(Sylvester, 1998). 此外, 这些样品还与区内同期的玄武岩样品具有近乎一致的形成年龄和相类似的 Sr-Nd-Hf 同

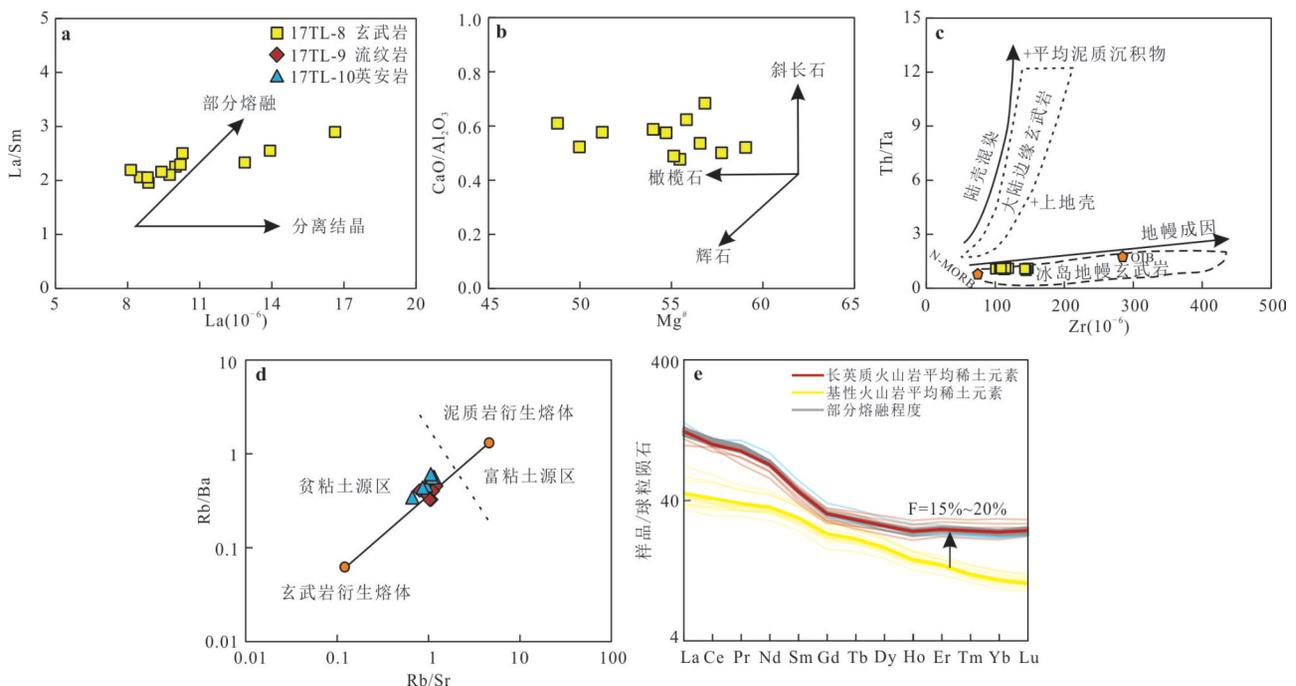


图 7 泰国东南部黎府带火山岩 La-La/Sm (a)、 $\text{Mg}^\#$ -CaO/ Al_2O_3 (b)、Zr-Th/Ta (c)、Rb/Sr-Rb/Ba(d)和部分熔融程度(e)模拟图解

Fig.7 Plots of La-La/Sm (a), $\text{Mg}^\#$ -CaO/ Al_2O_3 (b), Zr-Th/Ta (c), Rb/Sr-Rb/Ba (d) and partial melting degree simulation (e) for the volcanic rocks in the Loei zone of SE Thailand

图 c 据 Liu *et al.* (2021); 图 d 据 Sylvester (1998)

位素组成,这些特征表明这套长英质火山岩可能具有与该套玄武岩相类似的源区特征.本文基于平衡部分熔融模型进行模拟,选取了玄武岩样品的稀土元素均值作为固相母岩,而本套长英质火山岩样品的稀土元素均值落在玄武岩部分熔融程度为15%~20%的范围中(图7e),这一结果表明黎府带长英质火山岩可以是该套新底侵的基性岩经15%~20%低程度部分熔融而形成.

4.2 构造意义

东南亚地区已有的放射虫古生物记录、岩石年代学结果、地球化学及地质野外观测资料表明古特提斯洋在晚二叠世至早三叠世期间持续向东俯冲,并在早三叠世(~237 Ma)左右最终闭合,发生由古特提斯洋闭合向滇缅马与印支陆块碰撞的构造转换(如 Feng *et al.*, 2004; Ito *et al.*, 2016; Wang *et al.*, 2018; Yu *et al.*, 2023).这之后出露的火山岩及同期碎屑锆石普遍存在两期年龄峰值,表明在中一晚三叠世(~237~230 Ma),东南亚主要陆块拼合导致了地壳增厚,并沿着古特提斯缝合带发生了同碰撞的岩浆作用(如 Peng *et al.*, 2013; Qian *et al.*, 2016a, 2016b, 2017a).之后在晚三叠世(~230~200 Ma),发生板片断离及造山带垮塌,引起软流圈上涌从而导致了大规模的碰撞后岩浆作用的发生,并在泰国、柬埔寨、马来半岛等地区形成了以中部和东部花岗岩省为代表的碰撞后花岗岩(图8a;如 Searle *et al.*, 2012; Oliver *et al.*, 2014; Wang *et al.*, 2016; Uchida *et al.*, 2023; 余永琪等, 2024).而本文研究的泰国东南部黎府带内玄武岩和长英质火山岩的形成时代为晚三叠世(204~200 Ma),在时代上属于碰撞后阶段,且与区域上临沧及庄他武里—东马来以及柬埔寨地区碰撞后岩浆作用的形成时代相一致(如 Peng *et al.*, 2006; Wang *et al.*, 2010; Dong *et al.*, 2013; Qian *et al.*, 2017b; Uchida *et al.*, 2022, 2023; 余永琪等, 2024).此外,玄武岩和长英质火山岩具有相似的亏损的Sr-Nd-Hf同位素组成,部分熔融模拟结果表明长英质火山岩可能来源于新底侵的基性岩经低程度部分熔融而形成,这些特征也与双峰式火山岩的组合相类似(如 Davies and Macdonald., 1987; Frisch *et al.*, 2000; Li *et al.*, 2021).

如前所述,黎府带玄武岩和长英质火山岩样品分别具有富铌玄武岩和A型特征,地球化学特征也表明它们分别来自具有OIB特征的亏损地幔源区

和新底侵基性岩的部分熔融.一般富铌玄武岩的形成通常与局部或区域的伸展背景相联系,这种伸展作用可以是弧后盆地伸展,也可以是碰撞后伸展或裂谷背景(如 Brown *et al.*, 2002; Wang *et al.*, 2010; Liu *et al.*, 2017).在弧后伸展背景下富铌玄武岩通常表现出E-MORB的地球化学特征且具有Nb和Ta的负异常,同时具有较为亏损的同位素组成(如 Cawood and Williams, 1988; Fan *et al.*, 2010; Liu *et al.*, 2021).而本文研究的玄武岩样品形成于碰撞后阶段,且具有明显的Nb和Ta正异常(图5a和5b),这些特征与弧后盆地背景的起源不相符(如 Qian *et al.*, 2016b).在地球化学判别图解(图9a)中,玄武岩样品也分布在板内玄武岩区域.此外具有A型特征的长英质火山岩也同样形成于地壳减薄的伸展背景,根据构造背景的差异进一步分为A1型和A2型两类(Eby, 1990, 1992),其中A1型指示裂谷或板内的非造山背景,A2型指示碰撞后的伸展背景.在地球化学判别图解中(图4e),本文研究样品落入A2型区域,而在Rb-(Y+Nb)图解中(图9b),样品集中落入碰撞后背景区域内.此外区域的地质资料表明,泰国的三叠纪地层中发育有包含浅海沉积物的地堑盆地(如 Ridd *et al.*, 2011),这些特征进一步说明该套类似双峰式的火山岩可能形成于碰撞后伸展背景.如前所述在中一晚三叠世,印支陆块与滇缅马陆块发生碰撞导致岩石圈因挤压而缩短增厚,而这之后发生板片断离及造山带垮塌,促使软流圈地幔上涌,形成了区域内呈带状展布的碰撞后火山岩系列,如临沧—素可泰—庄他武里带内的花岗岩体及相关火山岩,其形成时代也主要集中在230~200 Ma(Barr *et al.*, 2000, 2006; Srichan *et al.*, 2009; Wang *et al.*, 2010, 2016; Qian *et al.*, 2013, 2016a, 2017b, 2022).此外,在研究区接壤的柬埔寨地区也同样出露有200 Ma左右的花岗质岩石(如 Uchida *et al.*, 2023),均证实了在晚三叠世晚期该区还存在大量的岩浆作用.因此,本研究认为随着软流圈的上涌,在研究区形成了一套具有OIB特征的富铌基性岩,同时促使这套新底侵的基性岩发生低程度的部分熔融从而形成了本研究中的长英质火山岩(图10).

泰国区域内发育了大规模与古特提斯演化相关的火成岩,它们的岩浆记录可从石炭纪追溯至三叠纪,本文将已发表的与黎府带及其周缘火山岩带相关的年代学数据进行了汇总表明黎府带最早的

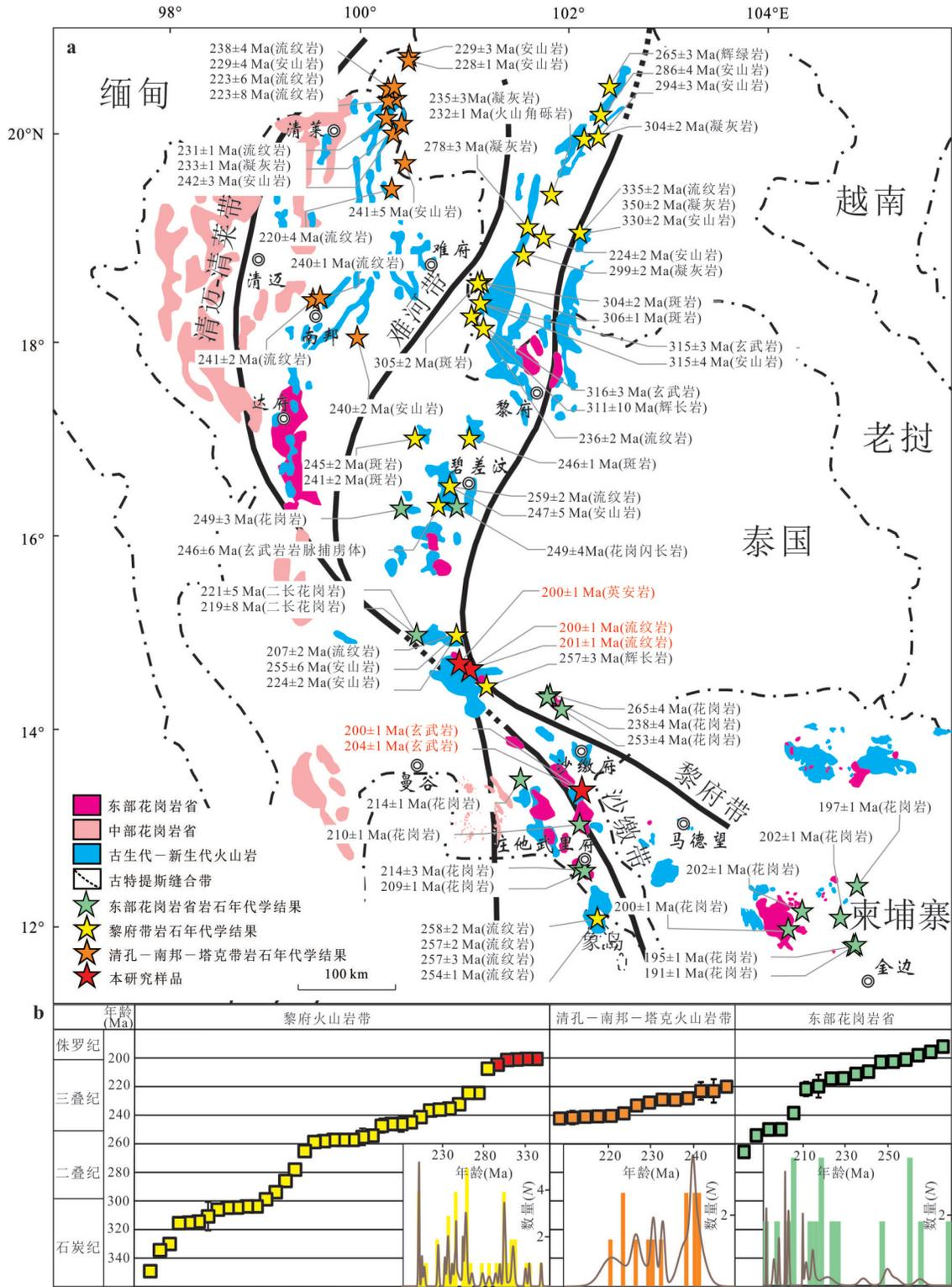


图 8 黎府带及其邻区火成岩年龄分布图(a)和年龄频谱图(b)

Fig.8 The distribution (a) and spectrogram (b) of formation ages for the igneous rocks along the Loie zone and surrounding areas
年代学数据来自 Barr *et al.* (2000, 2006); Srichan *et al.* (2009); Qian *et al.* (2013, 2015, 2016a, 2016b, 2017a, 2021, 2022); Kamvong *et al.* (2014); Salam *et al.* (2014); Arboit *et al.* (2016); Fanka *et al.* (2016, 2018); Yang *et al.* (2016); Shi *et al.* (2019, 2021); Wang *et al.* (2020), Nualkhao *et al.* (2018); Uchida *et al.* (2022, 2023)和本研究

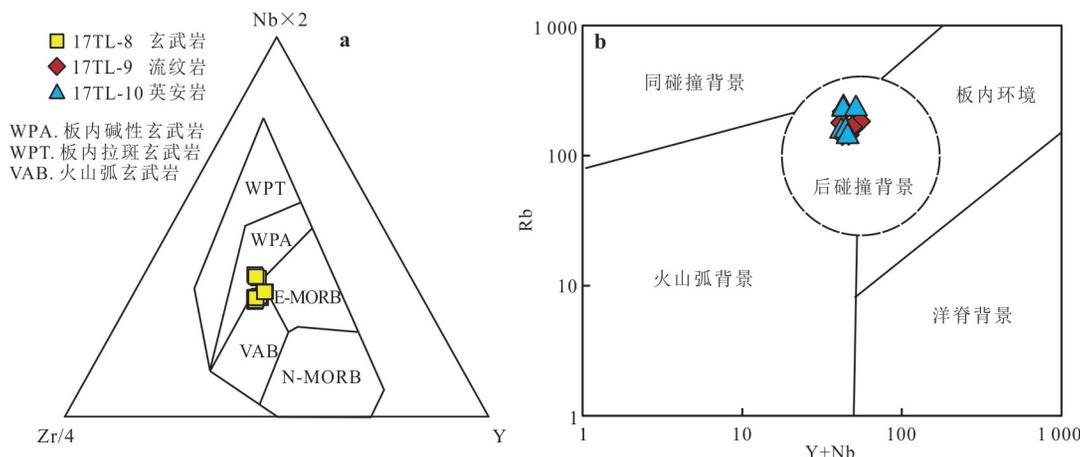


图9 泰国东南部黎府带火山岩构造环境判别图

Fig.9 Tectonic discrimination diagrams for the volcanic rocks in the Loei zone of SE Thailand

图 a 据 Meschede (1986); 图 b 据 Pearce et al. (1996)

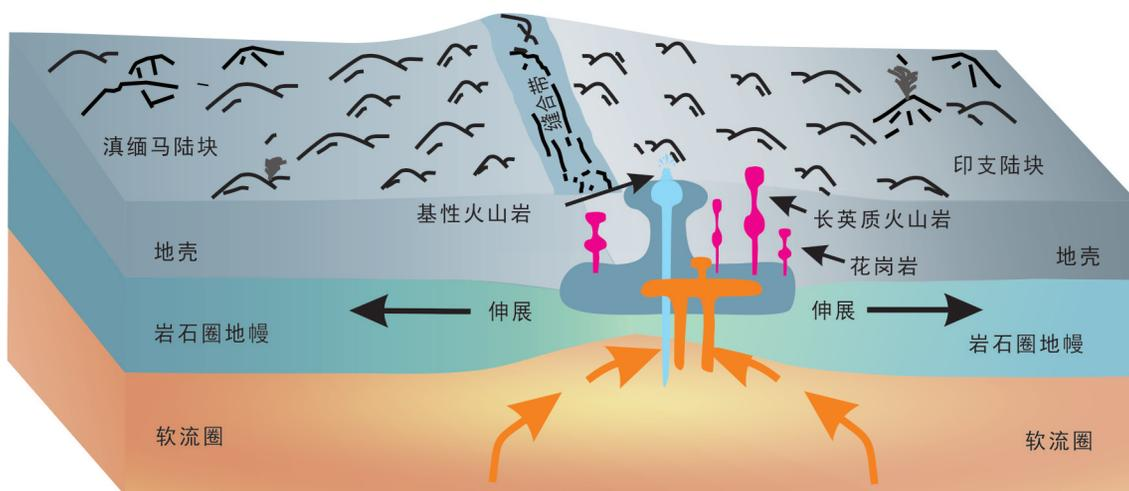


图 10 东古特提斯晚三叠世后碰撞伸展背景岩浆活动示意图

Fig.10 Tectonic cartoon showing the Paleotethyan extensional regime following the post-collision during the Late Triassic

岩浆作用记录主要集中在 350~304 Ma 或更早,并一直持续至中三叠世(图 8a; Kamvong *et al.*, 2014; Qian *et al.*, 2015; Yang *et al.*, 2016; Shi *et al.*, 2021).其中岛弧岩浆作用则主要分布在泰国境内黎府至碧差汶地区,年龄集中在 278~241 Ma (Kamvong *et al.*, 2014; Salam *et al.*, 2014; Fanka *et al.*, 2016; Shi *et al.*, 2019; Wang *et al.*, 2020; Qian *et al.*, 2022).在老挝地区出露的部分 237~232 Ma 的火山岩被解释为同碰撞岩浆作用的产物 (Shi *et al.*, 2019, 2021).而泰国 Khao Khwang 褶皱带地区出露的 224~207 Ma 的火山岩和泰国东南部及柬埔寨西部地区出露的 232~191 Ma 花岗岩均被解释为碰撞后岩浆作用的产物 (Arboit *et al.*, 2016; Uchida *et al.*, 2022, 2023).而本文研究的泰国东南

部黎府带火山岩的形成时代为约 200 Ma,是该构造带内最晚期的岩浆记录,同时也是东古特提斯洋闭合后最末期的岩浆作用.此外通过区域内的对比和分析发现,黎府带与素可泰地区清孔-南邦-塔克火山岩带具有相类似的三叠纪年龄谱系(图 8b),证实了黎府带在中-晚三叠世时期也同样记录了碰撞及碰撞后的岩浆作用.

5 结论

(1) 泰国东南部黎府带玄武岩和长英质火山岩的锆石 U-Pb 定年为 204~200 Ma,均形成于晚三叠世,区内构成类似双峰式组合.

(2) 泰国东南部黎府带晚三叠世火山岩具有相似的 Sr-Nd-Hf 同位素组成,其中玄武岩样品源自具

OIB 特征的亏损地幔源区, 而长英质火山岩可能源自该套新底侵基性岩的低程度部分熔融。

(3) 泰国东南部黎府带晚三叠世火山岩形成于东古特提斯碰撞后的伸展背景, 为东古特提斯洋碰撞闭合后最晚期的岩浆作用。

附件资料见地球科学官网: <https://doi.org/10.3799/dqkx.2024.112>

References

- Aguillón-Robles, A., Calmus, T., Benoit, M., et al., 2001. Late Miocene Adakites and Nb-Enriched Basalts from Vizcaino Peninsula, Mexico: Indicators of East Pacific Rise Subduction below Southern Baja California? *Geology*, 29(6): 531–534. [https://doi.org/10.1130/0091-7613\(2001\)029<0531:lmaane>2.0.co;2](https://doi.org/10.1130/0091-7613(2001)029<0531:lmaane>2.0.co;2)
- Arboit, F., Collins, A.S., Morley, C.K., et al., 2016. Geochronological and Geochemical Studies of Mafic and Intermediate Dykes from the Khao Khwang Fold-Thrust Belt: Implications for Petrogenesis and Tectonic Evolution. *Gondwana Research*, 36: 124–141. <https://doi.org/10.1016/j.jgr.2016.04.005>
- Barr, S.M., Charusiri, P., 2011. Volcanic Rocks. In: Ridd, M.F., ed., *The Geology of Thailand*. Geological Society of London, London. <https://doi.org/10.1144/goth.15>
- Barr, S.M., MacDonald, A.S., Dunning, G.R., et al., 2000. Petrochemistry, U-Pb (Zircon) Age, and Palaeotectonic Setting of the Lampang Volcanic Belt, Northern Thailand. *Journal of the Geological Society*, 157(3): 553–563. <https://doi.org/10.1144/jgs.157.3.553>
- Barr, S.M., MacDonald, A.S., Ounchanum, P., et al., 2006. Age, Tectonic Setting and Regional Implications of the Chiang Khong Volcanic Suite, Northern Thailand. *Journal of the Geological Society*, 163(6): 1037–1046. <https://doi.org/10.1144/0016-76492005-118>
- Blichert-Toft, J., Albarède, F., 1997. The Lu-Hf Isotope Geochemistry of Chondrites and the Evolution of the Mantle-Crust System. *Earth and Planetary Science Letters*, 148(1–2): 243–258. [https://doi.org/10.1016/s0012-821x\(97\)00040-x](https://doi.org/10.1016/s0012-821x(97)00040-x)
- Brown, S.J.A., Barley, M.E., Krapež, B., et al., 2002. The Late Archaean Melita Complex, Eastern Goldfields, Western Australia: Shallow Submarine Bimodal Volcanism in a Rifted Arc Environment. *Journal of Volcanology and Geothermal Research*, 115(3–4): 303–327. [https://doi.org/10.1016/s0377-0273\(01\)00314-6](https://doi.org/10.1016/s0377-0273(01)00314-6)
- Bunopas, S., 1981. Paleogeographic History of Western Thailand and Adjacent Parts of Southeast Asia: A Plate Tectonic Interpretation. Department of Mineral Resources of Thailand, Bangkok, Thailand. *Geological Survey of Thailand, Special Paper*, 5: 1–810.
- Castillo, P.R., 2008. Origin of the Adakite-High-Nb Basalt Association and Its Implications for Postsubduction Magmatism in Baja California, Mexico. *GSA Bulletin*, 120(3–4): 451–462. <https://doi.org/10.1130/b26166.1>
- Cawood, P.A., Johnson, M.R.W., Nemchin, A.A., 2007. Early Palaeozoic Orogenesis along the Indian Margin of Gondwana: Tectonic Response to Gondwana Assembly. *Earth and Planetary Science Letters*, 255(1–2): 70–84. <https://doi.org/10.1016/j.epsl.2006.12.006>
- Cawood, P.A., Williams, H., 1988. Acadian Basement Thrusting, Crustal Delamination, and Structural Styles in and around the Humber Arm Allochthon, Western Newfoundland. *Geology*, 16(4): 370–373. [https://doi.org/10.1130/0091-7613\(1988\)0160370:abtcd>2.3.co;2](https://doi.org/10.1130/0091-7613(1988)0160370:abtcd>2.3.co;2)
- Chairangsee, C., Hinze, C., Machareonsap, S., et al., 1990. Geological Map of Thailand 1:50 000—Explanation for the Sheets 5345 II (Amphoe Pak Chom), 5344 I (Ban Na Kho), 5445 III (Ban Huai Khop) and 5444 IV (King Amphoe Nam Som). *Geologisches Jahrbuch Reihe B*, 73: 3–55.
- Charusiri, P., Clark, A.H., Farrar, E., et al., 1993. Granite Belts in Thailand: Evidence from the $^{40}\text{Ar}/^{39}\text{Ar}$ Geochronological and Geological Syntheses. *Journal of Southeast Asian Earth Sciences*, 8(1–4): 127–136. [https://doi.org/10.1016/0743-9547\(93\)90014-g](https://doi.org/10.1016/0743-9547(93)90014-g)
- Charusiri, P., Daorerk, V., Archibald, D., et al., 2002. Geotectonic Evolution of Thailand: A New Synthesis. *Journal of the Geological Society of Thailand*, 1: 1–20.
- Collins, W.J., Beams, S.D., White, A.J.R., et al., 1982. Nature and Origin of A-Type Granites with Particular Reference to Southeastern Australia. *Contributions to Mineralogy and Petrology*, 80(2): 189–200. <https://doi.org/10.1007/bf00374895>
- Davies, G.R., MacDonald, R., 1987. Crustal Influences in the Petrogenesis of the Naivasha Basalt—Comendite Complex: Combined Trace Element and Sr-Nd-Pb Isotope Constraints. *Journal of Petrology*, 28(6): 1009–1031. <https://doi.org/10.1093/petrology/28.6.1009>
- Dong, G.C., Mo, X.X., Zhao, Z.D., et al., 2013. Zircon U-Pb Dating and the Petrological and Geochemical Constraints on Lincang Granite in Western Yunnan, China: Implications for the Closure of the Paleo-Tethys Ocean. *Journal of Asian Earth Sciences*, 62: 282–294. <https://doi.org/10.1016/j.jseas.2012.10.003>
- Eby, G.N., 1990. The A-Type Granitoids: A Review of Their

- Occurrence and Chemical Characteristics and Speculations on Their Petrogenesis. *Lithos*, 26(1-2): 115-134. [https://doi.org/10.1016/0024-4937\(90\)90043-z](https://doi.org/10.1016/0024-4937(90)90043-z)
- Eby, G.N., 1992. Chemical Subdivision of the A-Type Granitoids: Petrogenetic and Tectonic Implications. *Geology*, 20(7): 641-644. [https://doi.org/10.1130/0091-7613\(1992\)0200641:csotat>2.3.co;2](https://doi.org/10.1130/0091-7613(1992)0200641:csotat>2.3.co;2)
- Fan, J.J., Zhang, B.C., Zhou, J.B., et al., 2024. The Meso-Tethys Ocean: The Nature, Extension and Spatial-Temporal Evolution. *Earth - Science Reviews*, 255: 104839. <https://doi.org/10.1016/j.earsci-rev.2024.104839>
- Fan, W.M., Wang, Y.J., Zhang, A.M., et al., 2010. Permian Arc-back-Arc Basin Development along the Ailaoshan Tectonic Zone: Geochemical, Isotopic and Geochronological Evidence from the Mojiang Volcanic Rocks, Southwest China. *Lithos*, 119(3-4): 553-568. <https://doi.org/10.1016/j.lithos.2010.08.010>
- Fanka, A., Tsunogae, T., Daorerk, V., et al., 2016. Petrochemistry and Mineral Chemistry of Late Permian Hornblende and Hornblende Gabbro from the Wang Nam Khiao Area, Nakhon Ratchasima, Thailand: Indication of Palaeo-Tethyan Subduction. *Journal of Asian Earth Sciences*, 130: 239-255. <https://doi.org/10.1016/j.jseas.2016.11.018>
- Fanka, A., Tsunogae, T., Daorerk, V., et al., 2018. Petrochemistry and Zircon U-Pb Geochronology of Granitic Rocks in the Wang Nam Khiao Area, Nakhon Ratchasima, Thailand: Implications for Petrogenesis and Tectonic Setting. *Journal of Asian Earth Sciences*, 157: 92-118. <https://doi.org/10.1016/j.jseas.2017.08.025>
- Feng, Q.L., Chonglakmani, C., Helmcke, D., et al., 2004. Long-Lived Paleotethyan Pelagic Remnant inside Shan-Thai Block: Evidence from Radiolarian Biostratigraphy. *Science in China: Earth Sciences*, 47(12): 1113-1119. <https://doi.org/10.1360/03yd0085>
- Feng, Q.L., Chonglakmani, C., Ingavat-Helmcke, R., 2009. Evolution of the Loei Fold Belt in Northeastern Thailand and Northwestern Laos. *Acta Geoscientica Sinica*, 30(Suppl.1): 9. <https://doi.org/10.3975/cagsb.2009.s1.06>
- Feng, Q.L., Yang, W.Q., Shen, S.Y., et al., 2008. The Permian Seamount Stratigraphic Sequence in Chiang Mai, North Thailand and Its Tectogeographic Significance. *Science in China: Earth Sciences*, 51(12): 1768-1775. <https://doi.org/10.1007/s11430-008-0121-5>
- Frisch, W., Dunkl, I., Kuhlemann, J., 2000. Post-Collisional Orogen-Parallel Large-Scale Extension in the Eastern Alps. *Tectonophysics*, 327(3-4): 239-265. [https://doi.org/10.1016/s0040-1951\(00\)00204-3](https://doi.org/10.1016/s0040-1951(00)00204-3)
- Frost, C.D., Ronald Frost, B., 1997. Reduced Rapakivi-Type Granites: The Tholeiite Connection. *Geology*, 25(7): 647-650. [https://doi.org/10.1130/0091-7613\(1997\)0250647:rrtgtt>2.3.co;2](https://doi.org/10.1130/0091-7613(1997)0250647:rrtgtt>2.3.co;2)
- Griffin, W.L., Powell, W.J., Pearson, N.J., et al., 2008. Appendix A2: Glitter: Data Reduction Software for Laser Ablation ICP-MS. In: Sylvester, P., ed., *Laser Ablation ICP-MS in the Earth Sciences: Current Practices and Outstanding Issues*. Mineralogical Association of Canada, Canada, 308-311. <https://doi.org/10.3749/9780921294801.app02>
- Guo, L.N., Deng, J., Hou, L., et al., 2024. Gold Source and Deposition in the Sanakham Gold Deposit, SW Laos: Constrains from Textures, Trace Element Geochemistry and In-Situ Sulfur Isotopes of Pyrite. *Ore Geology Reviews*, 167: 106003. <https://doi.org/10.1016/j.oregeorev.2024.106003>
- Hara, H., Charoentitirat, T., Tokiwa, T., et al., 2024. Record of the Indosinian Orogeny from Conglomerates and Detrital Zircon U-Pb Ages of the Western Indochina Block, Central Thailand. *Gondwana Research*, 128: 368-389. <https://doi.org/10.1016/j.gr.2023.11.009>
- Hastie, A.R., Kerr, A.C., Pearce, J.A., et al., 2007. Classification of Altered Volcanic Island Arc Rocks Using Immobile Trace Elements: Development of the Th-Co Discrimination Diagram. *Journal of Petrology*, 48(12): 2341-2357. <https://doi.org/10.1093/petrology/egm062>
- Hu, Z.C., Liu, Y.S., Gao, S., et al., 2012. Improved *in situ* Hf Isotope Ratio Analysis of Zircon Using Newly Designed X Skimmer Cone and Jet Sample Cone in Combination with the Addition of Nitrogen by Laser Ablation Multiple Collector ICP-MS. *Journal of Analytical Atomic Spectrometry*, 27(9): 1391-1399. <https://doi.org/10.1039/c2ja30078h>
- Hutchison, C.S., Tan, D.N.K., 2009. *Geology of Peninsular Malaysia*. The University of Malaya and the Geological Society of Malaysia, Kuala Lumpur.
- Ito, T., Qian, X., Feng, Q.L., 2016. Geochemistry of Triassic Siliceous Rocks of the Muyinhe Formation in the Changning-Menglian Belt of Southwest China. *Journal of Earth Science*, 27(3): 403-411. <https://doi.org/10.1007/s12583-016-0672-x>
- Jin, J.J., Qian, X., Senebottalath, V., et al., 2024. Provenance and Paleogeographic Evolution of The Upper Paleozoic-Lower Mesozoic Strata in Northern Laos. *Journal of Earth Science*. <https://doi.org/10.1007/s12583-024-0011-6>

- Kamvong, T., Zaw, K., Meffre, S., et al., 2014. Adakites in the Truong Son and Loei Fold Belts, Thailand and Laos: Genesis and Implications for Geodynamics and Metallogeny. *Gondwana Research*, 26(1): 165–184. <https://doi.org/10.1016/j.gr.2013.06.011>
- Kepezhinskas, P., Defant, M.J., Drummond, M.S., 1996. Progressive Enrichment of Island Arc Mantle by Melt-Peridotite Interaction Inferred from Kamchatka Xenoliths. *Geochimica et Cosmochimica Acta*, 60(7): 1217–1229. [https://doi.org/10.1016/0016-7037\(96\)00001-4](https://doi.org/10.1016/0016-7037(96)00001-4)
- Kerr, A., Fryer, B.J., 1993. Nd Isotope Evidence for Crust-Mantle Interaction in the Generation of A-Type Granitoid Suites in Labrador, Canada. *Chemical Geology*, 104(1–4): 39–60. [https://doi.org/10.1016/0009-2541\(93\)90141-5](https://doi.org/10.1016/0009-2541(93)90141-5)
- King, P.L., White, A.J.R., Chappell, B.W., et al., 1997. Characterization and Origin of Aluminous A-Type Granites from the Lachlan Fold Belt, Southeastern Australia. *Journal of Petrology*, 38(3): 371–391. <https://doi.org/10.1093/ptro/38.3.371>
- Le Maitre, R.W., 1989. A Classification of Igneous Rocks and Glossary of Terms: Recommendations of the International Union of Geological Sciences Subcommittee on the Systematics of Igneous Rocks. International Union of Geological Sciences, Blackwell, Oxford.
- Li, H.L., Qian, X., Yu, X.Q., et al., 2023. Petrogenesis of Triassic Granites from Kontum Massif in Vietnam and Its Tethyan Tectonic Implications. *Earth Science*, 48(4): 1441–1460 (in Chinese with English abstract).
- Li, Y.X., Yin, C.Q., Lin, S.F., et al., 2021. Geochronology and Geochemistry of Bimodal Volcanic Rocks from the Western Jiangnan Orogenic Belt: Petrogenesis, Source Nature and Tectonic Implication. *Precambrian Research*, 359: 106218. <https://doi.org/10.1016/j.precamres.2021.106218>
- Liu, C.S., Chen, X.M., Chen, P.R., et al., 2003. Subdivision, Discrimination Criteria and Genesis for a Type Rock Suites. *Geological Journal of China Universities*, 9(4): 573–591 (in Chinese with English abstract).
- Liu, G.C., Li, J., Qian, X., et al., 2021. Geochronological and Geochemical Constraints on the Petrogenesis of Late Mesoproterozoic Mafic and Granitic Rocks in the Southwestern Yangtze Block. *Geoscience Frontiers*, 12(1): 39–52. <https://doi.org/10.1016/j.gsf.2020.07.005>
- Liu, H.C., Wang, Y.J., Cawood, P.A., et al., 2017. Episodic Slab Rollback and Back-Arc Extension in the Yunnan-Burma Region: Insights from Cretaceous Nb-Enriched and Oceanic-Island Basalt-Like Mafic Rocks. *Geological Society of America Bulletin*, 129(5–6): 698–714. <https://doi.org/10.1130/b31604.1>
- Ludwig, K.R., 2001. Using Isoplot/EX, Version 2.49. A Geochronological Toolkit for Microsoft Excel. Berkeley Geochronological Center Special Publications, Berkeley.
- Meschede, M., 1986. A Method of Discriminating between Different Types of Mid-Ocean Ridge Basalts and Continental Tholeiites with the Nb-Zr-Y Diagram. *Chemical Geology*, 56(3–4): 207–218. [https://doi.org/10.1016/0009-2541\(86\)90004-5](https://doi.org/10.1016/0009-2541(86)90004-5)
- Metcalfe, I., 1996. Gondwanaland Dispersion, Asian Accretion and Evolution of Eastern Tethys. *Australian Journal of Earth Sciences*, 43(6): 605–623. <https://doi.org/10.1080/08120099608728282>
- Metcalfe, I., 2000. The Bentong-Raub Suture Zone. *Journal of Asian Earth Sciences*, 18(6): 691–712. [https://doi.org/10.1016/s1367-9120\(00\)00043-2](https://doi.org/10.1016/s1367-9120(00)00043-2)
- Metcalfe, I., 2002. Permian Tectonic Framework and Palaeogeography of SE Asia. *Journal of Asian Earth Sciences*, 20(6): 551–566. [https://doi.org/10.1016/s1367-9120\(02\)00022-6](https://doi.org/10.1016/s1367-9120(02)00022-6)
- Metcalfe, I., 2006. Palaeozoic and Mesozoic Tectonic Evolution and Palaeogeography of East Asian Crustal Fragments: The Korean Peninsula in Context. *Gondwana Research*, 9(1–2): 24–46. <https://doi.org/10.1016/j.gr.2005.04.002>
- Metcalfe, I., 2011. Palaeozoic-Mesozoic History of SE Asia. *Geological Society, London, Special Publications*, 355(1): 7–35. <https://doi.org/10.1144/sp355.2>
- Metcalfe, I., 2013. Gondwana Dispersion and Asian Accretion: Tectonic and Palaeogeographic Evolution of Eastern Tethys. *Journal of Asian Earth Sciences*, 66: 1–33. <https://doi.org/10.1016/j.jseaes.2012.12.020>
- Metcalfe, I., 2021. Multiple Tethyan Ocean Basins and Orogenic Belts in Asia. *Gondwana Research*, 100: 87–130. <https://doi.org/10.1016/j.gr.2021.01.012>
- Mingram, B., Trumbull, R.B., Littman, S., et al., 2000. A Petrogenetic Study of Anorogenic Felsic Magmatism in the Cretaceous Paresis Ring Complex, Namibia: Evidence for Mixing of Crust and Mantle-Derived Components. *Lithos*, 54(1–2): 1–22. [https://doi.org/10.1016/s0024-4937\(00\)00033-5](https://doi.org/10.1016/s0024-4937(00)00033-5)
- Namur, O., Charlier, B., Toplis, M.J., et al., 2011. Differentiation of Tholeiitic Basalt to A-Type Granite in the Sept Îles Layered Intrusion, Canada. *Journal of Petrology*, 52(3): 487–539. <https://doi.org/10.1093/ptrology/egq088>
- Nie, Z.T., Liang, D.Y., Song, Z.M., et al., 1997. Discovery of

- Permian Pro-Gondwanan Facies in Western Margin of Simao Massif and Its Significance. *Geoscience*, 11(3): 261–267(in Chinese with English abstract).
- Nualkhao, P., Takahashi, R., Imai, A., et al., 2018. Petrochemistry of Granitoids along the Loei Fold Belt, Northeastern Thailand. *Resource Geology*, 68(4):395–424. <https://doi.org/10.1111/rge.12176>
- Oliver, G., Zaw, K., Hotson, M., et al., 2014. U-Pb Zircon Geochronology of Early Permian to Late Triassic Rocks from Singapore and Johor: A Plate Tectonic Reinterpretation. *Gondwana Research*, 26(1): 132–143. <https://doi.org/10.1016/j.gr.2013.03.019>
- Pearce, J., 1996. Sources and Settings of Granitic Rocks. *Episodes*, 19(4): 120–125. <https://doi.org/10.18814/epi-ugs/1996/v19i4/005>
- Peng, T. P., Wang, Y. J., Fan, W. M., et al., 2006. SHRIMP Zircon U-Pb Geochronology of Early Mesozoic Felsic Igneous Rocks from the Southern Lancangjiang and Its Tectonic Implications. *Science in China (Series D)*, 49(10): 1032–1042. <https://doi.org/10.1007/s11430-006-1032-y>
- Peng, T. P., Wilde, S. A., Wang, Y. J., et al., 2013. Mid-Triassic Felsic Igneous Rocks from the Southern Lancangjiang Zone, SW China: Petrogenesis and Implications for the Evolution of Paleo-Tethys. *Lithos*, 168: 15–32. <https://doi.org/10.1016/j.lithos.2013.01.015>
- Plank, T., 2005. Constraints from Thorium/Lanthanum on Sediment Recycling at Subduction Zones and the Evolution of the Continents. *Journal of Petrology*, 46(5): 921–944. <https://doi.org/10.1093/petrology/egi005>
- Qian, X., Feng, Q. L., Chonglakmani, C., et al., 2013. Geochemical and Geochronological Constraints on the Chiang Khong Volcanic Rocks (Northwestern Thailand) and Its Tectonic Implications. *Frontiers of Earth Science*, 7(4): 508–521. <https://doi.org/10.1007/s11707-013-0399-2>
- Qian, X., Feng, Q. L., Wang, Y. J., et al., 2016a. Geochronological and Geochemical Constraints on the Mafic Rocks along the Luang Prabang Zone: Carboniferous Back-Arc Setting in Northwest Laos. *Lithos*, 245: 60–75. <https://doi.org/10.1016/j.lithos.2015.07.019>
- Qian, X., Feng, Q. L., Wang, Y. J., et al., 2016b. Petrochemistry and Tectonic Setting of the Middle Triassic Arc-Like Volcanic Rocks in the Sayabouli Area, NW Laos. *Journal of Earth Science*, 27(3): 365–377. <https://doi.org/10.1007/s12583-016-0669-5>
- Qian, X., Feng, Q. L., Wang, Y. J., et al., 2017a. Late Triassic Post-Collisional Granites Related to Paleotethyan Evolution in SE Thailand: Geochronological and Geochemical Constraints. *Lithos*, 286: 440–453. <https://doi.org/10.1016/j.lithos.2017.06.026>
- Qian, X., Wang, Y. J., Srithai, B., et al., 2017b. Geochronological and Geochemical Constraints on the Intermediate-Acid Volcanic Rocks along the Chiang Khong-Lampang-Tak Igneous Zone in NW Thailand and Their Tectonic Implications. *Gondwana Research*, 45: 87–99. <https://doi.org/10.1016/j.gr.2016.12.011>
- Qian, X., Feng, Q. L., Yang, W. Q., et al., 2015. Arc-Like Volcanic Rocks in NW Laos: Geochronological and Geochemical Constraints and Their Tectonic Implications. *Journal of Asian Earth Sciences*, 98: 342–357. <https://doi.org/10.1016/j.jseaes.2014.11.035>
- Qian, X., Ma, S., Lu, X. H., et al., 2022. Late Permian Ultrapotassic Rhyolites in SE Thailand: Evidence for a Palaeotethyan Continental Rift Basin. *Journal of the Geological Society*, 179(2): jgs2021–jgs2079. <https://doi.org/10.1144/jgs2021-079>
- Qian, X., Wang, Y. J., Zhang, Y. Z., et al., 2019. Petrogenesis of Permian-Triassic Felsic Igneous Rocks along the Truong Son Zone in Northern Laos and Their Paleotethyan Assembly. *Lithos*, 328: 101–114. <https://doi.org/10.1016/j.lithos.2019.01.006>
- Qian, X., Wang, Y. J., Zhang, Y. Z., et al., 2020. Late Triassic Post-Collisional Granites Related to Paleotethyan Evolution in Northwestern Lao PDR: Geochronological and Geochemical Evidence. *Gondwana Research*, 84: 163–176. <https://doi.org/10.1016/j.gr.2020.03.002>
- Qian, X., Wang, Y. J., Zhang, Y. Z., et al., 2021. Constraints of Late Triassic Mafic-Felsic Volcanic Rocks in Northwestern Laos on the Eastern Paleotethyan Post-Collisional Setting. *Journal of Asian Earth Sciences*, 218: 104889. <https://doi.org/10.1016/j.jseaes.2021.104889>
- Ridd, M. F., 2015. East Flank of the Sibumasu Block in NW Thailand and Myanmar and Its Possible Northward Continuation into Yunnan: A Review and Suggested Tectono-Stratigraphic Interpretation. *Journal of Asian Earth Sciences*, 104: 160–174. <https://doi.org/10.1016/j.jseaes.2014.01.023>
- Ridd, M. F., Barber, A. J., Crow, M. J., 2011. The Geology of Thailand. Geological Society of London, London. <https://doi.org/10.1144/goth>
- Salam, A., Zaw, K., Meffre, S., et al., 2014. Geochemistry and Geochronology of the Chatree Epithermal Gold-Silver Deposit: Implications for the Tectonic Setting of the Loei Fold Belt, Central Thailand. *Gondwana Research*, 26(1): 198–217. <https://doi.org/10.1016/j.gr.2013.10.008>
- Sashida, K., Igo, H., Hisafa, K. I., et al., 1993. Occurrence of

- Paleozoic and Early Mesozoic Radiolaria in Thailand (Preliminary Report). *Journal of Southeast Asian Earth Sciences*, 8(1–4): 97–108. [https://doi.org/10.1016/0743-9547\(93\)90011-d](https://doi.org/10.1016/0743-9547(93)90011-d)
- Scherer, E., Munker, C., Mezger, K., 2001. Calibration of the Lutetium-Hafnium Clock. *Science*, 293(5530): 683–687. <https://doi.org/10.1126/science.1061372>
- Searle, M.P., Whitehouse, M.J., Robb, L.J., et al., 2012. Tectonic Evolution of the Sibumasu-Indochina Terrane Collision Zone in Thailand and Malaysia: Constraints from New U-Pb Zircon Chronology of SE Asian Tin Granitoids. *Journal of the Geological Society*, 169(4): 489–500. <https://doi.org/10.1144/0016-76492011-107>
- Shi, M.F., Khin, Z., Liu, S.S., et al., 2021. Geochronology and Petrogenesis of Carboniferous and Triassic Volcanic Rocks in NW Laos: Implications for the Tectonic Evolution of the Loei Fold Belt. *Journal of Asian Earth Sciences*, 208: 104661. <https://doi.org/10.1016/j.jseaes.2020.104661>
- Shi, M.F., Wu, Z.B., Liu, S.S., et al., 2019. Geochronology and Petrochemistry of Volcanic Rocks in the Xaignabouli Area, NW Laos. *Journal of Earth Science*, 30(1): 37–51. <https://doi.org/10.1007/s12583-018-0863-8>
- Sone, M., Metcalfe, I., 2008. Parallel Tethyan Sutures in Mainland Southeast Asia: New Insights for Palaeo-Tethys Closure and Implications for the Indosinian Orogeny. *Comptes Rendus Geoscience*, 340(2–3): 166–179. <https://doi.org/10.1016/j.crte.2007.09.00>
- Sone, M., Metcalfe, I., Chaodumrong, P., 2012. The Chanthaburi Terrane of Southeastern Thailand: Stratigraphic Confirmation as a Disrupted Segment of the Sukhothai Arc. *Journal of Asian Earth Sciences*, 61: 16–32. <https://doi.org/10.1016/j.jseaes.2012.08.021>
- Song, P.P., Ding, L., Lippert, P.C., et al., 2020. Paleomagnetism of Middle Triassic Lavas from Northern Qiangtang (Tibet): Constraints on the Closure of the Paleo-Tethys Ocean. *Journal of Geophysical Research: Solid Earth*, 125(2): e2019JB017804. <https://doi.org/10.1029/2019jb017804>
- Srichan, W., Crawford, A.J., Berry, R.F., 2009. Geochemistry and Geochronology of Late Triassic Volcanic Rocks in the Chiang Khong Region, Northern Thailand. *Island Arc*, 18(1): 32–51. <https://doi.org/10.1111/j.1440-1738.2008.00660.x>
- Sun, S.S., McDonough, W.F., 1989. Chemical and Isotopic Systematics of Oceanic Basalts: Implications for Mantle Composition and Processes. *Geological Society, London, Special Publications*, 42(1): 313–345. <https://doi.org/10.1144/gsl.sp.1989.042.01.19>
- Sylvester, P.J., 1998. Post-Collisional Strongly Peraluminous Granites. *Lithos*, 45(1–4): 29–44. [https://doi.org/10.1016/s0024-4937\(98\)00024-3](https://doi.org/10.1016/s0024-4937(98)00024-3)
- Uchida, E., Nagano, S., Niki, S., et al., 2022. Geochemical and Radiogenic Isotopic Signatures of Granitic Rocks in Chanthaburi and Chachoengsao Provinces, Southeastern Thailand: Implications for Origin and Evolution. *Journal of Asian Earth Sciences: X*, 8: 100111. <https://doi.org/10.1016/j.jaesx.2022.100111>
- Uchida, E., Nagano, S., Niki, S., et al., 2023. U-Pb Dating for Zircons from Granitic Rocks in Southwestern Cambodia. *Heliyon*, 9(9): e19734. <https://doi.org/10.1016/j.heliyon.2023.e19734>
- Udchachon, M., Thassanapak, H., Burrett, C., et al., 2024. Microfacies and Palaeoenvironments of Late Cisuralian and Guadalupian (Early to Middle Permian) Alatoconchid-Bearing Limestone in Loei Fold Belt, Indochina Terrane. *Journal of Palaeogeography*, 13(3): 453–474. <https://doi.org/10.1016/j.jop.2024.03.003>
- Ueno, K., 2003. The Permian Fusulinoidean Faunas of the Sibumasu and Baoshan Blocks: Their Implications for the Paleogeographic and Paleoclimatologic Reconstruction of the Cimmerian Continent. *Palaeogeography, Palaeoclimatology, Palaeoecology*, 193(1): 1–24. [https://doi.org/10.1016/s0031-0182\(02\)00708-3](https://doi.org/10.1016/s0031-0182(02)00708-3)
- Ueno, K., Charoentitrat, T., 2011. Carboniferous and Permian. In: Ridd, M.F., Barber, A.J., Crow, M.J., eds., *The Geology of Thailand*. The Geological Society of London, London. <https://doi.org/10.1144/goth.5>
- Ueno, K., Hisada, K.I., 2001. The Nan-Uttaradit-Sa Kaeo Suture as a Main Paleo-Tethyan Suture in Thailand: Is It Real? *Gondwana Research*, 4(4): 804–806. [https://doi.org/10.1016/s1342-937x\(05\)70590-6](https://doi.org/10.1016/s1342-937x(05)70590-6)
- Vander Auwera, J., Bogaerts, M., Liégeois, J.P., et al., 2003. Derivation of the 1.0–0.9 Ga Ferro-Potassic A-Type Granitoids of Southern Norway by Extreme Differentiation from Basic Magmas. *Precambrian Research*, 124(2–4): 107–148. [https://doi.org/10.1016/s0301-9268\(03\)00084-6](https://doi.org/10.1016/s0301-9268(03)00084-6)
- Vervoort, J.D., Patchett, P.J., Blichert-Toft, J., et al., 1999. Relationships between Lu-Hf and Sm-Nd Isotopic Systems in the Global Sedimentary System. *Earth and Planetary Science Letters*, 168(1–2): 79–99. [https://doi.org/10.1016/s0012-821x\(99\)00047-3](https://doi.org/10.1016/s0012-821x(99)00047-3)
- Wang, Y.J., He, H.Y., Cawood, P.A., et al., 2016. Geochronological, Elemental and Sr-Nd-Hf-O Isotopic Constraints on the Petrogenesis of the Triassic Post-Collisional Gra-

- nitic Rocks in NW Thailand and Its Paleotethyan Implications. *Lithos*, 266:264–286. <https://doi.org/10.1016/j.lithos.2016.09.012>
- Wang, Y. J., He, H. Y., Zhang, Y. Z., et al., 2017. Origin of Permian OIB-Like Basalts in NW Thailand and Implication on the Paleotethyan Ocean. *Lithos*, 274: 93–105. <https://doi.org/10.1016/j.lithos.2016.12.021>
- Wang, Y. J., Lu, X. H., Qian, X., et al., 2022. Prototethyan Orogenesis in Southwest Yunnan and Southeast Asia. *Science China Earth Sciences*, 65(10): 1921–1947. <https://doi.org/10.1007/s11430-021-9958-7>
- Wang, Y. J., Qian, X., Cawood, P. A., et al., 2018. Closure of the East Paleotethyan Ocean and Amalgamation of the Eastern Cimmerian and Southeast Asia Continental Fragments. *Earth-Science Reviews*, 186: 195–230. <https://doi.org/10.1016/j.earscirev.2017.09.013>
- Wang, Y. J., Qian, X., Cawood, P. A., et al., 2021a. Prototethyan Accretionary Orogenesis along the East Gondwana Periphery: New Insights from the Early Paleozoic Igneous and Sedimentary Rocks in the Sibumasu. *Geochemistry, Geophysics, Geosystems*, 22(5): e2020GC009622. <https://doi.org/10.1029/2020gc009622>
- Wang, Y. J., Yang, T. X., Zhang, Y. Z., et al., 2020. Late Paleozoic Back-Arc Basin in the Indochina Block: Constraints from the Mafic Rocks in the Nan and Luang Prabang Tectonic Zones, Southeast Asia. *Journal of Asian Earth Sciences*, 195: 104333. <https://doi.org/10.1016/j.jseaes.2020.104333>
- Wang, Y. J., Zhang, A. M., Fan, W. M., et al., 2010. Petrogenesis of Late Triassic Post-Collisional Basaltic Rocks of the Lancangjiang Tectonic Zone, Southwest China, and Tectonic Implications for the Evolution of the Eastern Paleotethys: Geochronological and Geochemical Constraints. *Lithos*, 120(3–4): 529–546. <https://doi.org/10.1016/j.lithos.2010.09.012>
- Wang, Y. J., Zhang, Y. Z., Qian, X., et al., 2021b. Early Paleozoic Accretionary Orogenesis in the Northeastern Indochina and Implications for the Paleogeography of East Gondwana: Constraints from Igneous and Sedimentary Rocks. *Lithos*, 382: 105921. <https://doi.org/10.1016/j.lithos.2020.105921>
- Whalen, J. B., Currie, K. L., Chappell, B. W., 1987. A-Type Granites: Geochemical Characteristics, Discrimination and Petrogenesis. *Contributions to Mineralogy and Petrology*, 95(4): 407–419. <https://doi.org/10.1007/bf00402202>
- Wu, F. Y., Wan, B., Zhao, L., et al., 2020. Tethyan Geodynamics. *Acta Petrologica Sinica*, 36(6): 1627–1674 (in Chinese with English abstract).
- Xu, C., Wang, Y. J., Qian, X., et al., 2020. Geochronological and Geochemical Characteristics of Early Silurian S-Type Granitic Gneiss in Takengon Area of Northern Sumatra and Its Tectonic Implications. *Earth Science*, 45(6): 2077–2090 (in Chinese with English abstract).
- Yang, J. H., Wu, F. Y., Chung, S. L., et al., 2006. A Hybrid Origin for the Qianshan A-Type Granite, Northeast China: Geochemical and Sr-Nd-Hf Isotopic Evidence. *Lithos*, 89(1–2): 89–106. <https://doi.org/10.1016/j.lithos.2005.10.002>
- Yang, W. Q., Qian, X., Feng, Q. L., et al., 2016. Zircon U-Pb Geochronological Evidence for the Evolution of the Nan-Uttaradit Suture in Northern Thailand. *Journal of Earth Science*, 27(3): 378–390. <https://doi.org/10.1007/s12583-016-0670-z>
- Yin, A., Harrison, T. M., 2000. Geologic Evolution of the Himalayan-Tibetan Orogen. *Annual Review of Earth and Planetary Sciences*, 28: 211–280. <https://doi.org/10.1146/annurev.earth.28.1.211>
- Yu, X. Q., Qian, X., Lu, X. H., et al., 2021. Zircon U-Pb Geochronology of Late Triassic Granites from Sibolga Area in Western Sumatra and Its Tethyan Tectonic Implications. *Earth Science*, 46(8): 2873–2886 (in Chinese with English abstract).
- Yu, Y. Q., Qian, X., Azlan Mustapha, K., et al., 2022. Late Paleozoic-Early Mesozoic Granitic Rocks in Eastern Peninsular Malaysia: New Insights for the Subduction and Evolution of the Paleo-Tethys. *Journal of Asian Earth Sciences*, 239: 105427. <https://doi.org/10.1016/j.jseaes.2022.105427>
- Yu, Y. Q., Qian, X., Ghani, A. A., et al., 2023. Triassic Felsic Magmatism in SE Peninsular Malaysia: Petrogenesis and Geodynamic Implications for the Eastern Paleotethyan Tectonic Transition. *Lithos*, 462: 107399. <https://doi.org/10.1016/j.lithos.2023.107399>
- Yu, Y. Q., Qian, X., Wang, Y. J., et al., 2024. Late Triassic Magmatism in Eastern Peninsular Malaysia and Its Paleotethyan Tectonic Implications. *Geotectonica et Metallogenia*, 48(3): 493–511 (in Chinese with English abstract).
- Zhang, Q., Li, C. D., 2012. Granites: Implications for Continental Geodynamics. Ocean Press, Beijing (in Chinese).
- Zhang, Y. Z., Yu, X. Q., et al., 2023. Reconstructing the East Palaeo-Tethyan Assemblage Boundary in West Indonesia: Constraints from Triassic Granitoids in the Bangka and Belitung Islands. *Geological Society, London, Special Publications*, 531(1): 265–286. <https://doi.org/10.1144/sp531-2022-144>

- Zhang, Z.C., Wang, F.S., Hao, Y.L., et al., 2004. Geochemistry of the Picrites and Associated Basalts from the Emeishan Large Igneous Basalt Province and Constraints on Their Source Region. *Acta Geologica Sinica*, 78(2): 171–180 (in Chinese with English abstract).
- Zhang, Z.W., Shu, Q., Yang, X.Y., et al., 2019. Review on the Tectonic Terranes Associated with Metallogenic Zones in Southeast Asia. *Journal of Earth Science*, 30(1): 1–19. <https://doi.org/10.1007/s12583-019-0858-0>
- Zhao, T.Y., Qian, X., Feng, Q.L., 2016. Geochemistry, Zircon U-Pb Age and Hf Isotopic Constraints on the Petrogenesis of the Silurian Rhyolites in the Loei Fold Belt and Their Tectonic Implications. *Journal of Earth Science*, 27(3): 391–402. <https://doi.org/10.1007/s12583-016-0671-y>
- Zhong, D.L., 1998. The Gutethys Orogenic Belt in Western Yunnan and Sichuan. Science Press, Beijing (in Chinese).
- Zi, J.W., Cawood, P.A., Fan, W.M., et al., 2012. Generation of Early Indosinian Enriched Mantle-Derived Granitoid Pluton in the Sanjiang Orogen (SW China) in Response to Closure of the Paleo-Tethys. *Lithos*, 140: 166–182. <https://doi.org/10.1016/j.lithos.2012.02.006>
- 李慧玲, 钱鑫, 余小清, 等, 2023. 越南昆嵩地体三叠纪花岗岩岩石成因及其特提斯构造意义. *地球科学*, 48(4): 1441–1460.
- 刘昌实, 陈小明, 陈培荣, 等, 2003. A型岩套的分类、判别标志和成因. *高校地质学报*, 9(4): 573–591.
- 聂泽同, 梁定益, 宋志敏, 等, 1997. 早二叠世亲冈瓦纳相在思茅地块西缘的发现及其意义. *现代地质*, 11(3): 261–268.
- 吴福元, 万博, 赵亮, 等, 2020. 特提斯地球动力学. *岩石学报*, 36(6): 1627–1674.
- 徐畅, 王岳军, 钱鑫, 等, 2020. 苏门答腊岛北部 Takengon 早志留世 S型花岗片麻岩年代学、地球化学特征及构造意义. *地球科学*, 45(6): 2077–2090.
- 余小清, 钱鑫, 卢向红, 等, 2021. 西苏门答腊实武牙地区晚三叠世花岗岩锆石年代学及其特提斯构造意义. *地球科学*, 46(8): 2873–2886.
- 余永琪, 钱鑫, 王岳军, 等, 2024. 马来半岛东部晚三叠世岩浆作用及其古特提斯构造意义. *大地构造与成矿学*, 48(3): 493–511.
- 张旗, 李承东, 2012. 花岗岩地球动力学意义. 北京: 海洋出版社.
- 张招崇, 王福生, 郝艳丽, 等, 2004. 峨眉山大火成岩省中苦橄岩与其共生岩石的地球化学特征及其对源区的约束. *地质学报*, 78(2): 171–180.
- 钟大赟, 1998. 滇川西部古特提斯造山带. 北京: 科学出版社.

中文参考文献

李慧玲, 钱鑫, 余小清, 等, 2023. 越南昆嵩地体三叠纪花岗岩